

# TRIP12's role in the governance of DNA polymerase $\beta$ involvement in DNA damage response and repair

Burcu Inanc<sup>1,†</sup>, Qingming Fang<sup>2,3,4,†</sup>, Wynand P. Roos<sup>5</sup>, Joel F. Andrews<sup>2</sup>, Xuemei Zeng<sup>6</sup>, Jennifer Clark<sup>2,3</sup>, Jianfeng Li<sup>2,3,7</sup>, Nupur B. Dey<sup>2,3</sup>, Md Ibrahim<sup>2,3</sup>, Peter Sykora<sup>2,8</sup>, Zhongxun Yu<sup>9,10</sup>, Charlotte R. Pearson<sup>5</sup>, Andrea Braganza<sup>10</sup>, Marcel Verheij<sup>1,11,16</sup>, Jos Jonkers<sup>12</sup>, Nathan A. Yates<sup>6,13</sup>, Conchita Vens<sup>1,11,14,15,\*</sup>, Robert W. Sobol<sup>16,2,3,5,10,\*</sup>

<sup>1</sup>Division of Cell Biology, The Netherlands Cancer Institute, Amsterdam 1066CX, The Netherlands

<sup>2</sup>Mitchell Cancer Institute, University of South Alabama, Mobile, AL 36604, United States

<sup>3</sup>Department of Pharmacology, College of Medicine, University of South Alabama, Mobile, AL 36688, United States

<sup>4</sup>Present address: University of Texas Health Science Center at San Antonio, San Antonio, TX 78229, United States

<sup>5</sup>Department of Pathology and Laboratory Medicine, Warren Alpert Medical School & Legorreta Cancer Center, Brown University, Providence, RI 02912, United States

<sup>6</sup>Biomedical Mass Spectrometry Center, University of Pittsburgh, Pittsburgh, PA 15213, United States

<sup>7</sup>Present address: Department of Pharmacology and Chemical Biology, Emory University, Atlanta, GA 30322, United States

<sup>8</sup>Present address: Amelia Technologies, Washington, D.C. 20007, United States

<sup>9</sup>Department of Medicine, Tsinghua University School of Medicine, Tsinghua University, Haidian District, Beijing 100084, China

<sup>10</sup>Department of Pharmacology & Chemical Biology, University of Pittsburgh, Pittsburgh, PA 15213, United States

<sup>11</sup>Department of Radiation Oncology, The Netherlands Cancer Institute, Amsterdam 1066CX, The Netherlands

<sup>12</sup>Division of Molecular Pathology, The Netherlands Cancer Institute, Amsterdam 1066CX, The Netherlands

<sup>13</sup>Department of Cell Biology, University of Pittsburgh, Pittsburgh, PA 15261, United States

<sup>14</sup>School of Cancer Sciences, University of Glasgow, Glasgow G61 1QH, United Kingdom

<sup>15</sup>Department of Head and Neck Oncology and Surgery, Antoni van Leeuwenhoek Hospital, Amsterdam 1066CX, The Netherlands

<sup>16</sup>Present address: Department of Radiation Oncology, Radboud University Medical Centre, 6525 GA Nijmegen, The Netherlands

\*To whom correspondence should be addressed. Email: [rwsobol@brown.edu](mailto:rwsobol@brown.edu)

Correspondence may also be addressed to Conchita Vens. Email: [conchita.vens@glasgow.ac.uk](mailto:conchita.vens@glasgow.ac.uk)

†The first two authors should be regarded as Joint First Authors.

## Abstract

The multitude of DNA lesion types, and the nuclear dynamic context in which they occur, presents a challenge for genome integrity maintenance as this requires the engagement of different DNA repair pathways. Specific “repair controllers” that facilitate DNA repair pathway crosstalk between double-strand break (DSB) repair and base excision repair (BER) and that regulate BER protein engagement at lesion sites have yet to be identified. Here, we find that DNA polymerase  $\beta$  (Pol $\beta$ ), crucial for BER, is ubiquitinated in a BER complex-dependent manner by TRIP12, an E3 ligase that partners with UBR5 to restrain DSB repair signaling. Furthermore, we find that TRIP12, but not UBR5, controls cellular levels and chromatin loading of Pol $\beta$ . Required for Pol $\beta$  foci formation, TRIP12 influences Pol $\beta$  involvement after radiation-induced DNA damage, a process regulated by TRIP12-mediated ubiquitylation of Pol $\beta$ . Notably, excessive TRIP12-mediated engagement of Pol $\beta$  affects DSB formation and radiation sensitivity, underscoring its role in promoting precedence for BER over DSB repair. The herein discovered function of TRIP12, in the governance of Pol $\beta$ -directed BER, supports a role for TRIP12 in assuring BER lesion removal at complex DSB sites to optimize DSB repair at the nexus of DNA repair pathways.

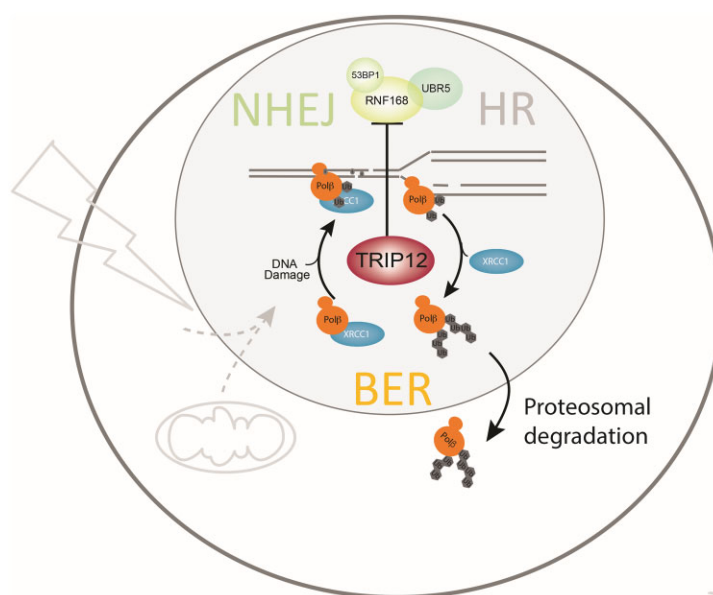
Received: April 12, 2024. Revised: May 12, 2025. Editorial Decision: May 13, 2025. Accepted: June 11, 2025

© The Author(s) 2025. Published by Oxford University Press on behalf of Nucleic Acids Research.

This is an Open Access article distributed under the terms of the Creative Commons Attribution-NonCommercial License

(<https://creativecommons.org/licenses/by-nc/4.0/>), which permits non-commercial re-use, distribution, and reproduction in any medium, provided the original work is properly cited. For commercial re-use, please contact [reprints@oup.com](mailto:reprints@oup.com) for reprints and translation rights for reprints. All other permissions can be obtained through our RightsLink service via the Permissions link on the article page on our site—for further information please contact [journals.permissions@oup.com](mailto:journals.permissions@oup.com).

## Graphical abstract



## Introduction

Genome integrity maintenance is challenged by the multitude of different DNA lesion types and the nuclear dynamic context in which they occur. Resolution of DNA damage caused by exogenous or endogenous sources requires the engagement of different DNA repair pathways. This is typically determined by the type of lesion and the cell cycle phase. DNA double-strand break (DSB) repair pathways are tightly regulated to ensure efficient repair in different cell cycle phases and chromatin conditions [1, 2]. Single-strand breaks (SSBs) and damaged bases are mainly repaired by DNA polymerase  $\beta$  (Pol $\beta$ )-dependent base excision repair (BER). In a previous study, we found that BER protein complex composition and protein stability change upon exposure to damage such as from radiation and in a cell cycle phase-dependent manner [3].

Complex DNA lesion sites that contain different lesions in close proximity pose particularly difficult repair conditions as they may require the involvement of intrinsically very distinct repair pathways. Thus, repair pathway choice and sequence are crucial to the success of DNA damage repair under such conditions. Nonhomologous end joining (NHEJ) and homologous recombination (HR) are the most prominent DSB repair options, and their interaction and relative contribution have been actively researched in recent years [4, 5]. DSBs, such as those caused by radiation or generated due to DNA crosslinks from metabolic formaldehyde, cisplatin, or similar crosslinkers, can create marked threats to DNA replication and cellular division. These potentially lethal lesions are resolved by DSB repair processes. BER, on the other hand, deals with base lesions or contributes to SSB repair (SSBR), abundantly generated by metabolic processes, reactive oxygen species, deamination, or depurination [6, 7]. Greatly outnumbering DSBs, radiation also causes a multitude of BER-specific lesion types [8, 9]. Of these, oxidative base lesions and SSBs are the most predominant. As such, radiation-induced DNA damage can be very complex in nature, comprised of a mixture of DNA lesions in close proximity requiring both DSB repair and BER.

Different DNA lesion types, when adjacent to each other, require proper spatiotemporal as well as chronological (or sequential) engagement of different repair proteins. In fact, radiation-induced complex DSBs, which also comprise multiple base damages, are the most difficult to repair and hence most detrimental to cellular survival and genomic integrity. The chromatin context in which those lesions occur is also an important factor in DNA damage repair that needs to consider replication, transcription, and different (hetero)chromatic conditions. Even though close links between distinct lesion repair pathways would be expected, no studies exist that demonstrate an inter-pathway collaboration of BER and DSB repair, and few report the involvement of individual BER elements in DSB repair processes [10–12]. Crosstalk mechanisms that enable DNA repair pathway choice at lesions and chromatin sites that are common to both, and the orchestration of protein complex formation thereof, remain elusive.

Chromatin and repair enzyme modifications by ubiquitylation are relevant processes that regulate the DNA damage response (DDR) and DSB repair [13]. An RNF8/RNF168 E3 ubiquitin ligase-coordinated cascade of non-proteolytic ubiquitylation events results in chromatin marks in the vicinity of DSBs. RNF168-dependent chromatin ubiquitylation mediates the accrual of the DSB repair proteins 53BP1 and BRCA1 to the lesion site [14], and additional studies have shown how RNF168-mediated 53BP1 engagement can support the regulation of DSB repair [15–17]. 53BP1 recruitment blocks resection, an important step in HR, to ultimately promote NHEJ. Resection and therefore HR, on the other hand, is facilitated by BRCA1 by counteracting 53BP1 recruitment at such ubiquitylated sites [18]. A recent report further supports a role for RNF168 in facilitating HR through PALB2 loading in a BRCA1-independent manner [19, 20]. Together, this highlights the intricate molecular mechanisms by which chromatin ubiquitylation directs DSB repair pathway choice. Surprisingly, to date no similar processes have been linked directly to BER/SSBR.

A different E3 ubiquitin ligase, TRIP12 (ULF), has also been shown to regulate DDR protein homeostasis. TRIP12 prevents 53BP1 hyperaccumulation by controlling RNF168 residence at break sites [21], thus indicating an involvement of TRIP12 in DSB repair suppression. TRIP12 was also reported to affect PARP inhibitor efficacy [22, 23] and to interact with Ku70 [24], while its expression was found to be regulated by p16 [25, 26]. Despite this and a reported effect on the USP7-regulated stabilization of p53 [27], little is known about TRIP12's overall impact on DNA repair and cellular functions.

Pol $\beta$  has a crucial function in BER and SSBR. Upon lesion recognition and removal by glycosylases and AP endonuclease 1, Pol $\beta$  executes end-tailoring and DNA synthesis at the gap [7]. The 5'dRP lyase and nucleotidyl transferase activities allow Pol $\beta$ , supported by XRCC1, to execute base and single-strand break repair in many cases [28]. The distinctive expression pattern of Pol $\beta$ , across different tissues and during development, points to processes that tightly regulate Pol $\beta$  protein levels, suggesting a requirement to assure context-appropriate BER and Pol $\beta$ -dependent activity [29]. Deregulated expression has indeed been reported to lead to interference in replication processes and defects in Pol $\beta$  subcellular localization resulting in altered damage response [30–35]. Such findings led us to postulate the existence of molecular and cellular mechanisms that counteract the dangers of such “over”-repair by stringently controlling Pol $\beta$  levels to exclude Pol $\beta$  from such disruptive activities. Our past studies revealed elements in the governance of Pol $\beta$  levels and stability that ultimately also define BER protein complex makeup. We elucidated the regulation of the BER/SSBR protein complex architecture through proteolytic ubiquitylation events and HSP90 binding via its interaction with XRCC1 in response to damage [3]. In this earlier study [3], we showed that separation-of-function mutants of Pol $\beta$  failed to interact with XRCC1 and were targeted for ubiquitylation and degradation. A knock-in mouse model expressing such a separation-of-function mutant of Pol $\beta$  confirmed reduced Pol $\beta$  protein levels *in vivo* [36]. Importantly, we also found that the proliferation status of the cell and the nature of the damaging agent defined BER complex formation and Pol $\beta$  stability [3]. Solely in proliferating cells and distinctively different from the BER complex formation pattern observed after alkylating agents, radiation exposure led to increased levels of the HSP90-bound XRCC1 [3]. These data led us to hypothesize that BER/SSBR protein complex formation is context dependent and can vary according to cell cycle phase or DNA damage type. Two ubiquitylation sites on Pol $\beta$  suggested an unidentified regulatory component of BER/SSBR. We, therefore, searched for a ubiquitin ligase that fulfills this role in Pol $\beta$  regulation and discovered how this new element in BER/SSBR (TRIP12) provides a “repair-controller” function.

## Materials and methods

### Materials

All materials and supplies are listed in [Supplementary Table S1](#).

### Cellular models

Cell line models were developed by lentivirus-mediated transduction of the glioma cell line LN428 to allow expression

of the indicated proteins (Flag-Pol $\beta$ , myc-TRIP12, copGFP-Pol $\beta$ ), as indicated in detail in [Supplementary Document S1](#) and [Supplementary Table S1](#). LN428 cells were chosen here as an extension of our previous work [3], demonstrating that the ubiquitylation of Pol $\beta$  is dependent on the interaction between Pol $\beta$  and XRCC1 [3]. In some cases, modified cells were further modified by a second transduction, such as expressing TRIP12-shRNA in cells modified for expression of Flag-Pol $\beta$ , and using lentiviral vectors with different selection makers (puromycin, geneticin, hygromycin). Flag-Pol $\beta$ , myc-TRIP12, myc-TRIP12-HECT, and myc-TRIP12-SB vectors were mainly used to assess binding interactions or ubiquitylation assays, as indicated throughout. CopGFP-Pol $\beta$ -based models were generated for laser-induced micro-irradiation experiments, radiation- or cisplatin-induced foci analysis, and nuclear colocalization analyses. For overexpression models, cell lines were developed with elevated Flag-Pol $\beta$  expression and respective mutants. Several different TRIP12 shRNA-based vectors were used to establish the cellular role of TRIP12 expression in Pol $\beta$  stability and radiation response.

### Methods

Detailed methods are described in [Supplementary Document S1](#).

In brief, standard cell lysis, chromatin fraction isolation, immunostaining, immunoblotting (IB), and immunofluorescence microscopy procedures were applied using the antibodies and conditions as indicated in the figures and legends and detailed in [Supplementary Document S1](#) and [Supplementary Table S1](#).

For protein complex partner identification and immunoprecipitation (IP), anti-Flag M2 affinity gel was used to immunoprecipitate the individual proteins after cell lysis with Pierce IP lysis buffer and according to the manufacturer's protocols. Twenty-seven individual IP samples were prepared ( $n = 9$  per condition) and loaded onto SDS-PAGE (sodium dodecyl sulfate–polyacrylamide gel electrophoresis) gels for label-free differential mass spectrometry (dMS) analysis. Tryptic peptides extracted from each IP product were separated by reverse-phased nano-flow liquid chromatography (EASY-nLC II, Thermo Scientific, San Jose, CA) and analyzed on an LTQ/Orbitrap Velos Elite hybrid mass spectrometer (Thermo Fisher, San Jose, CA). Mass spectrometry data collected for each sample were analyzed using dMS software (Infoclinika, Bellevue, WA). The high-resolution full MS spectra were aligned and the  $m/z$ , charge state, retention time, and intensity data for all molecular features detected in the full-scan mass spectra were integrated and matched to protein identification results as detailed in [Supplementary Document S1](#). Student's *t*-test implemented in MATLAB® was used to determine the statistical significance of the difference in the abundance of identified proteins/features in different IP samples. The abundance values in Flag-Pol $\beta$ (WT) and Flag-Pol $\beta$ (TM) samples were normalized to the Pol $\beta$  level in each sample to calculate the WT/TM ratio used to assess the differential interaction between Flag-Pol $\beta$ (WT) and Flag-Pol $\beta$ (TM) samples.

Recombinant proteins (His-tagged ubiquitin, His-Ub) were generated as detailed in [Supplementary Table S1](#) and [Supplementary Document S1](#). To study interactions with TRIP12 or ubiquitylation of Pol $\beta$ , IPs were performed using anti-TRIP12, anti-Myc, and anti-Pol $\beta$  (Clone 61) antibodies ([Supplementary Table S1](#)) as indicated in the figures



and following standard protocols (Supplementary Document S1). To assess the ubiquitylation activities of TRIP12 and the HECT or substrate binding (SB) domains of TRIP12, myc-TRIP12, myc-HECT, myc-HECT(C2007A), and myc-TRIP12-SB were immunoprecipitated using an anti-myc antibody or Myc-Trap agarose and exposed to *in vitro* ubiquitylation assays (Supplementary Document S1) with or without purified Pol $\beta$ . Ubiquitylation of purified Pol $\beta$  was examined after gel electrophoresis and IB with anti-Pol $\beta$  (Clone 61), anti-ubiquitin, and anti-His-tag antibodies. Autoubiquitylation of the TRIP12-HECT domain was examined after gel electrophoresis and IB as described above with an anti-ubiquitin or anti-His-tag antibody (Supplementary Document S1).

For Pol $\beta$  stability and degradation evaluation, cells were seeded and treated with 0.2 mM cycloheximide (Cyc) or with Cyc (0.2 mM) and MG132 (25  $\mu$ M) for the time indicated in the figures.

Radiation sensitivity and H<sub>2</sub>O<sub>2</sub>-induced cytotoxicity were determined using the colony formation assay as described in Supplementary Document S1. The CometChip assay was used to assess DNA damage and repair kinetics, as outlined in Supplementary Document S1.

### Statistical analysis

The statistical analysis procedures and parameters for the different analyses are described in Supplementary Document S1.

In brief, averages and standard deviations (SDs) were calculated from the means (of technical replicates) of multiple independent experiments ( $n$  = number of independent experiments as indicated in figure legends), unless stated otherwise. ANOVA was used to test for significant differences, generally compared to controls and as indicated in the figure legends. To enable the evaluation of potential changes in the distribution of the foci number per cell values, foci dot plots are shown and contain pooled foci data from all independent experiments, with a minimum of 50 analyzed cells for each experiment. A non-parametric test (Kruskal–Wallis with Dunn’s multiple comparison test) was used if the data did not pass the normality test. To evaluate robustness of the findings across multiple experiments, a second analysis considers the interexperimental variation and compares the means of the individual experiments using ANOVA after calculating the average and SD of the mean foci number per cell values derived from the independent experiments (Supplementary Document S1). Results of both analyses are shown throughout, either in the main or in the supplementary figures.

As the dependence of the individual data points in the survival dose response data precludes ANOVA analyses, nonlinear regressions were computed using  $Y = 100/[1 + (X^{\text{HillSlope}})/(IC_{50}^{\text{HillSlope}})]$  (with  $Y$  = survival in % and  $X$  = H<sub>2</sub>O<sub>2</sub> concentration) on the normalized H<sub>2</sub>O<sub>2</sub> dose response survival data to calculate IC<sub>50</sub> (half-maximal inhibitory concentration) values for each individual experiment. Similarly,  $D_{37}$  (radiation dose permitting 37% cell survival) values were calculated from linear quadratic fits [ $Y = \exp(-\alpha \cdot X - \beta \cdot X^2)$ , with  $X$  = radiation dose and  $Y$  = surviving fraction] on the survival curves. One-way ANOVA was then used to test for significant differences in these response parameter values as stated in the text.  $P$ -values are indicated by asterisks with \* $P$  < .05, \*\* $P$  < .01, \*\*\* $P$  < .001, and \*\*\*\* $P$  < .0001.

## Results

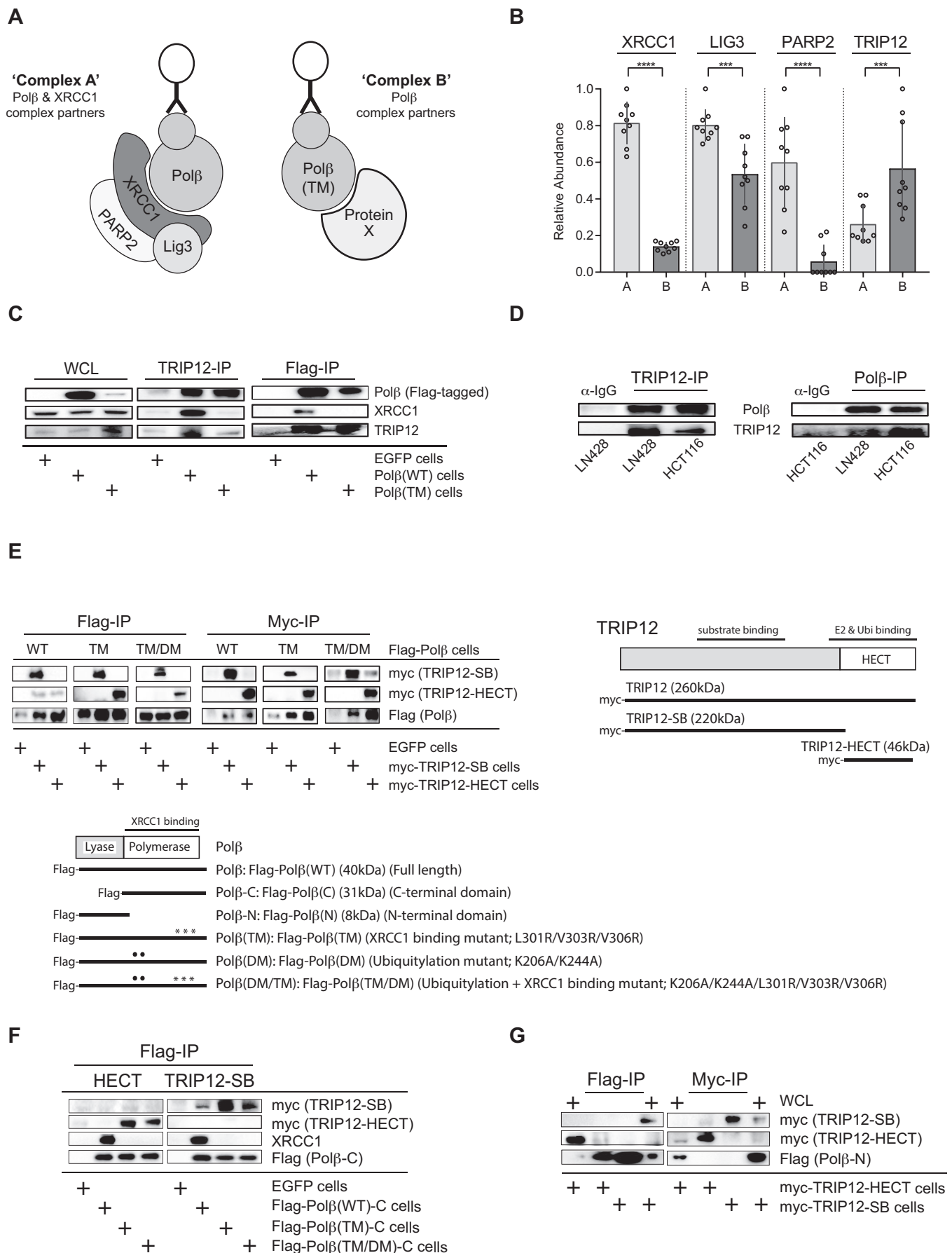
### DDR suppressor TRIP12 is a novel partner of the BER protein Pol $\beta$

The majority of Pol $\beta$  partners with XRCC1 to conduct BER [37]. Yet, XRCC1 and Pol $\beta$  function independently, in different BER subcomplexes, for yet undefined roles in DNA metabolism [3]. We recapitulated these main cellular BER complexes (herein termed Complex A, comprised of Pol $\beta$  and XRCC1, and Complex B, XRCC1-devoid complexes) by exploiting a separation-of-function mutant of Pol $\beta$  that does not bind to XRCC1, the V303-loop mutant Pol $\beta$ (TM), encoding the Pol $\beta$  mutations L301R/V303R/V306R (Supplementary Fig. S1A). This approach allowed us to reveal novel partners of Pol $\beta$  that are not dependent on XRCC1 (Fig. 1A). Using label-free dMS, an unbiased quantitative proteomic method [38, 39], we discovered TRIP12, a DSB repair-related E3 ubiquitin ligase, as a novel Pol $\beta$  partner. We found TRIP12 to bind preferentially to the Pol $\beta$ -centered Complex B, suggesting involvement in BER complex regulation (Fig. 1B, Supplementary Fig. S1B and C, and Supplementary Table S2). Pol $\beta$ (TM) cellular levels drop significantly (Supplementary Fig. S1B and C), as also reported previously [3]. The dMS analyses and IP experiments show that TRIP12 is bound to both Pol $\beta$ (WT) and Pol $\beta$ (TM), yet we observed a significantly increased interaction with Pol $\beta$ (TM) (Fig. 1B and Supplementary Fig. S1C). Other novel partners selectively bound to Pol $\beta$ (TM) include RFC1, EIF, BCKDHA, SPT16, and SSRP1 (Supplementary Table S2 and Supplementary Fig. S1D). Quantitative dMS and immunoprecipitation/immunoblot (IP/IB) analysis confirms the lack of XRCC1 and known XRCC1-mediated BER factors (LIG3, PARP2, PNKP, Aprataxin) in the Pol $\beta$ (TM) samples, supporting Pol $\beta$  specificity of the approach, and points to the dominance of TRIP12 among non-BER proteins in both the transgenic and endogenous setting and in different cell lines (Fig. 1C and D, and Supplementary Fig. 1C–E). Domain mapping of the interaction between the TRIP12 E3 ubiquitin ligase active site HECT domain and the remaining N-terminal E3 ubiquitin ligase SB domain (TRIP12-SB) shows Pol $\beta$  binding at TRIP12-SB and a preferential binding to the TRIP12-HECT and TRIP12-SB domains in the Pol $\beta$ -centric Complex B as revealed by the interaction with Pol $\beta$ (TM) (Fig. 1E–G and Supplementary Fig. S1F). This binding is mediated by the C-terminus of Pol $\beta$  that also binds to XRCC1 and contains the ubiquitylation target sites [K206, K244; mutated to alanine in Pol $\beta$ (DM)] [3].

### TRIP12 ubiquitylates Pol $\beta$ and targets it for degradation

The interaction of TRIP12 with Pol $\beta$  and its complex-selective nature suggest a role for TRIP12 as the primary E3 ubiquitin ligase regulating the observed cell cycle and DNA damage type-dependent stability of Pol $\beta$  [3, 37]. We therefore determined whether TRIP12 ubiquitylates Pol $\beta$  and whether this TRIP12-mediated ubiquitylation depends on the previously identified lysine residues (K206/K244) [3]. An *in vitro* “on-bead” assay [40–43] was designed to test TRIP12’s ability to ubiquitylate purified recombinant Pol $\beta$  and revealed evidence of prominent (mono- and poly-)ubiquitylated species.

As depicted in the “on-bead” Ubi-assay graphic (Fig. 2A, left), myc-tagged full-length TRIP12, TRIP12-HECT domain (WT or encoding the active site mutant C2007A), TRIP12



SB domain (TRIP12-SB), or EGFP (serving as negative control) was expressed in LN428 cells. Captured on beads (FR1 in [Supplementary Fig. S2A](#), left), these myc-tagged proteins were then incubated with recombinant His-tagged ubiquitin (FR2) and recombinant Pol $\beta$  (WT or the DM mutant, K206A/K244A) (in FR3) to compare TRIP12-mediated ubiquitylation of both Pol $\beta$  variants (Fig. 2A and B, and [Supplementary Fig. S2A](#)). HECT domain E3 ubiquitin ligases, and thus also TRIP12, first form a covalent intermediate (as depicted in FR2) before the ubiquitin is transferred to its substrate (in FR3) [41–43], as we also observed in previous UBE3B “on-bead Ubi-assay” analyses [40]. Here, we found that full-length TRIP12 and the HECT domain are both covalently modified by ubiquitin in this *in vitro* “on-bead” assay ([Supplementary Fig. S2A](#), right). Importantly, Pol $\beta$  (bound to the myc-tagged protein and beads in FR3, or released in FR4) is ubiquitylated in the presence of full-length TRIP12, or the TRIP12-HECT domain (Fig. 2A, right, and B). This ubiquitylation is impaired when the HECT domain active site is mutated (C2007A) as demonstrated by the lack of larger and modified Pol $\beta$  forms and greatly reduced mono-ubiquitylated forms (Fig. 2A, right, and B, right).

*In vivo* evaluation of the ubiquitylation of Pol $\beta$  was accomplished by expressing HA-tagged ubiquitin in Flag-tagged Pol $\beta$  (WT and mutants) expressing LN428 cells. IP of Flag-tagged Pol $\beta$ , followed by immunoblot for HA, confirmed TRIP12-dependent (poly-)ubiquitylation. Consistent with its preference to bind to BER Complex B (Fig. 1), this is increased in the triple mutant Pol $\beta$ (TM), which does not bind XRCC1 (Fig. 2C and [Supplementary Fig. S2C](#)). TRIP12-dependent (poly-)ubiquitylation is abrogated when modifying the potential ubiquitylation target sites in the Pol $\beta$ (TM/DM) and Pol $\beta$ (DM) mutants (Fig. 2C and [Supplementary Fig. S2B](#)) or when Flag-Pol $\beta$  is not expressed ([Supplementary Fig. S2C](#), right). Consistent with its proposed function [44], we observed binding of the TRIP12-HECT domain to ubiquitylated Pol $\beta$  in these IP experiments ([Supplementary Fig. S2C](#)).

Loss of XRCC1 binding results in five-fold decreased basal levels of Pol $\beta$  mutants that do not bind to XRCC1, such as Pol $\beta$ (TM) (as previously shown in [3]). Importantly, addition of the K206A/K244A mutations, Pol $\beta$ (TM/DM), however, reverts this instability phenotype [3]. Here, we find that TRIP12 affects Pol $\beta$  levels, revealing its role in this Pol $\beta$  degradation route (Fig. 2D). Underlining a complex-specific (and XRCC1-dependent) activity, loss of TRIP12 stabilizes Pol $\beta$ (TM) most profoundly (Fig. 2D and [Supplementary Fig. S2D](#) and E). These comparative expression analyses show that this effect on Pol $\beta$  protein levels is dependent on the potential ubiquitylation target sites K206/K244 [mutated in Pol $\beta$ (DM) and Pol $\beta$ (TM/DM)] (Fig. 2D), despite similarly efficient bind-

ing to full-length TRIP12 ([Supplementary Fig. S1F](#)). As also shown in our previous report [3], if bound to XRCC1 (Complex A) in undamaged cells, the wild-type version of Pol $\beta$ , Pol $\beta$ (WT), is stable and not subjected to proteasomal degradation within a 6-h time frame ([Supplementary Fig. S2F](#), left panel, Flag-Pol $\beta$ (WT), and G). Conversely, Pol $\beta$  is rapidly degraded if unable to bind to XRCC1 [3] ([Supplementary Fig. S2F](#), right panel, Flag-Pol $\beta$ (TM), and G). We further show that this degradation of (XRCC1-free) Pol $\beta$  is regulated by TRIP12 through the loss of such proteasome-mediated degradation processes in TRIP12-shRNA expressing cells ([Supplementary Fig. S2F](#) and G).

### TRIP12's impact on base excision repair processes

Supporting its nuclear role, TRIP12 mostly resides in the nucleus and on chromatin (Fig. 3A and B) [45, 46]. We find that, despite overall increased levels, the chromatin-associated fraction of endogenous Pol $\beta$  is reduced in TRIP12-shRNA expressing cells, suggesting that TRIP12 promotes Pol $\beta$  chromatin association (Fig. 3B). Furthermore, mutations of the Pol $\beta$  K206/K244 ubiquitylation sites greatly reduces chromatin, but not nuclear, localization of such transgenic Pol $\beta$  variants [Pol $\beta$ (DM) versus Pol $\beta$ (WT) in [Supplementary Fig. S3A](#)] indicating a role for TRIP12-mediated ubiquitylation in this process. This prompted us to investigate TRIP12's role in BER beyond an influence on BER complex-specific Pol $\beta$  degradation.

At the chromatin level, TRIP12 has been reported to prevent excessive DNA damage signaling and DSB repair protein accumulation to contain the cellular response to DSBs [21]. After confirming that TRIP12 depletion also affects RNF168 levels in our cellular models ([Supplementary Fig. S3B](#)), we first questioned whether TRIP12 affects Pol $\beta$ 's primary function in BER or affects BER overall. For this, we tested two BER-specific outcomes: (i) recruitment to sites of laser-induced DNA damage and (ii) response to and repair of oxidative and alkylation DNA damage. Our previous studies showed that Pol $\beta$  is recruited to sites of laser-induced DNA damage in a manner that depends on PARP1 activation and binding to XRCC1 [3, 5]. To test a potential impact on this BER process, here we compared copGFP-tagged Pol $\beta$  recruitment parameters in TRIP12-depleted cells to those in parental or scrambled shRNA (SCR)-expressing cells. We find that recruitment or retention of Pol $\beta$  at laser-induced DNA damage sites is not significantly affected by the presence or absence of TRIP12 (ANOVA  $P = .2-.65$ ; Fig. 3C and [Supplementary Fig. S3C](#)). Next, we evaluated whether the reduction of TRIP12 levels affects alkylation or oxidative damage repair as determined by alkaline DNA comet analysis using the CometChip

← affinity to the XRCC1-free complex (Complex B). Quantification of selected proteins bound to Complex A or Complex B, as indicated, by label-free dMS. The relative abundances of prototypic peptides with unique amino acid sequences AIGSTSKPOESPK, SEAHTADGISIR, VNNGNTAPEDSSPAK, and LSTQSNNSNIEPAR were used as surrogate measures of XRCC1, LIG3, PARP2, and TRIP12, respectively. Peptide abundance levels were normalized to Pol $\beta$  in each immunoprecipitated sample and are shown as dots on bar plots with mean and SD. Significant differences between complexes A and B are marked by asterisks (\*\* $P < .001$ , \*\*\*\* $P < .0001$ ; ANOVA). (C) BER complex-dependent interaction of TRIP12. Interaction of TRIP12 with Flag-Pol $\beta$ (WT) or Flag-Pol $\beta$ (TM) was revealed by IP from whole cell lysates (WCLs) and IB as indicated. (D) Interaction of endogenous Pol $\beta$  with TRIP12. IP/IB of endogenous proteins in the indicated cell lines are shown. (E) Domain interaction mapping. Flag-Pol $\beta$  binding to myc-TRIP12 domains as depicted in the scheme shown to the right and determined by IP/IB: myc-TRIP12 (full length TRIP12, with an N-terminal myc-tag), myc-TRIP12-SB (TRIP12 SB domain, amino acids 1–1650, with an N-terminal myc-tag), and myc-TRIP12-HECT (TRIP12-HECT domain, amino acids 1651–2040, with an N-terminal myc-tag). (F) Domain interaction mapping of myc-TRIP12 to the C-terminal domain of Pol $\beta$  wild-type and mutants by IP/IB: Flag-Pol $\beta$ (WT)-C (amino acids 91–335), Flag-Pol $\beta$ (TM)-C, XRCC1 binding mutant (amino acids 91–335), and Flag-Pol $\beta$ (TM/DM)-C, ubiquitylation and XRCC1 binding mutant (amino acids 91–335). (G) Domain interaction mapping of myc-TRIP12 to the N-terminal domain of Pol $\beta$  wild-type and mutants by IP/IB: Flag-Pol $\beta$ (WT)-N (amino acids 1–90).

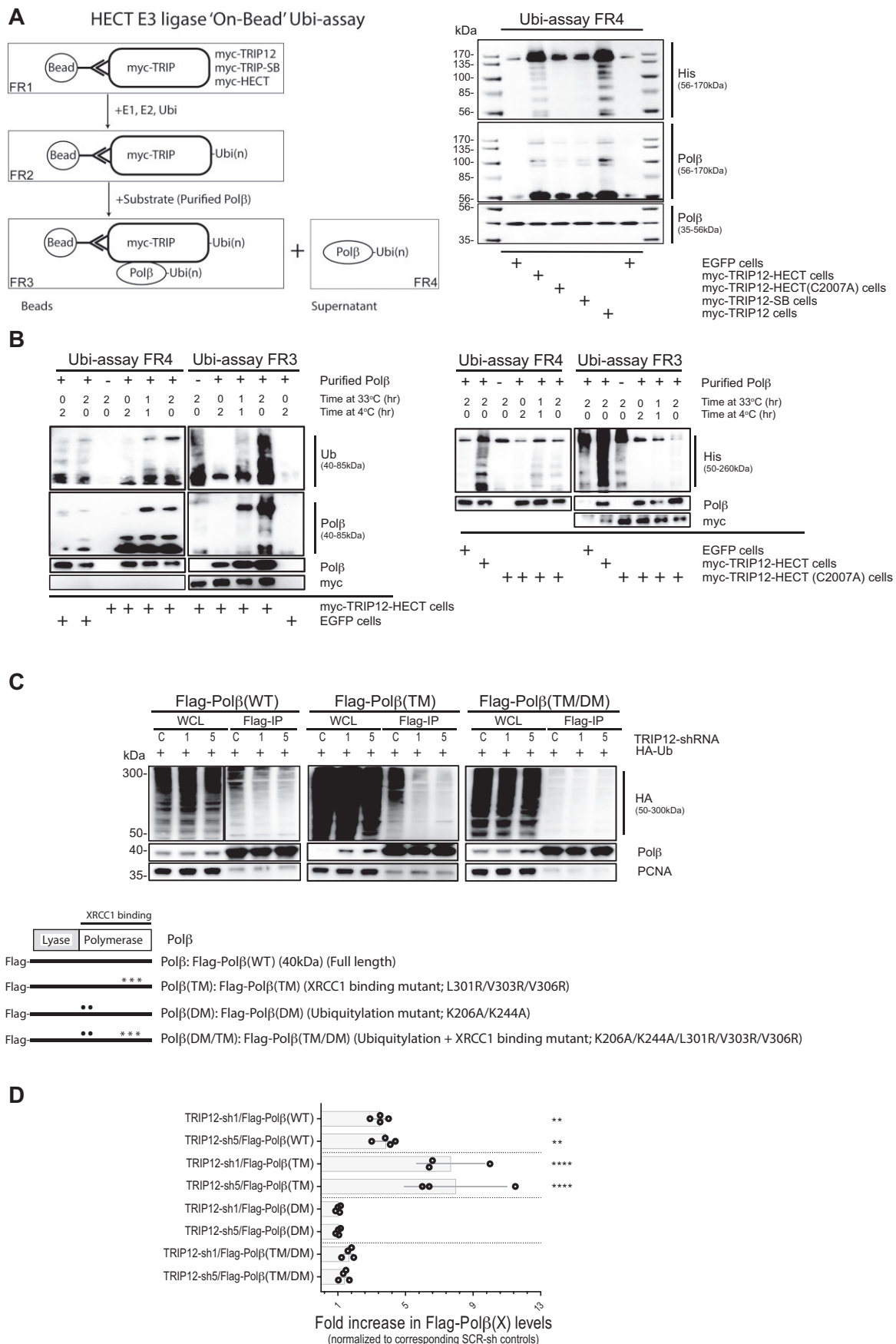


**Figure 2.** TRIP12's role in Polβ ubiquitylation and degradation. (A) *Ex vivo* Polβ ubiquitylation by TRIP12. Polβ ubiquitylation by TRIP12 as identified by immunoblot (right) after the "on-bead" Ubi- assay as outlined in the scheme (left) using recombinant and purified His-ubiquitin, E1/E2, and Polβ together



[47] or survival analyses. We, however, do not find significant changes in damage levels or survival that would support a role for TRIP12 as an essential factor to efficiently execute oxidative or alkylation damage repair (Fig. 3D and E, and [Supplementary Fig. S3D](#)). We then evaluated a potential role for TRIP12's involvement in cellular fitness and found that loss of TRIP12 does not affect proliferation or survival (Fig. 3F and G). Overall, TRIP12 does not appear to be essential for canonical BER activities or cell fitness, or its loss is compensated for by other regulators.

### TRIP12 facilitates Polβ engagement after radiation

Polβ has also been reported to participate in noncanonical BER-like processes in DSB repair. We previously reported that XRCC1-dependent functions of Polβ differ and depend on damage type and proliferation status, thereby linking BER protein complex makeup to a radiation damage and a replication context [3]. We observed enhanced HSP90/XRCC1 binding after radiation in proliferating cells that consequently promotes the Polβ-centric Complex B (XRCC1-free), herein observed to be preferred by TRIP12 (Fig. 1) [3]. This prompted an assessment of the Polβ response to radiation. Here, we find that after exposing cells to radiation, Polβ has both a rapid and persistent focal appearance in a radiation dose (thus DNA damage load)-dependent manner that indicates involvement in radiation-induced DNA damage repair (Fig. 4A–C and [Supplementary Fig. S4A](#) and B) [7]. Colocalization analyses show that this radiation-induced recruitment of Polβ is accompanied by the BER scaffold protein XRCC1 (Fig. 4D). The data show that the majority of Polβ(WT) foci colocalize with XRCC1 foci in control and irradiated cells. Radiation induction levels are comparable (mean of 3.1 versus  $2.6 \pm 0.8$  foci at 5 h) [3]. Radiation-induced changes in mean XRCC1 foci numbers are also similar to those in Polβ foci (1.32-fold with  $SD = 0.11$  versus 1.17-fold with  $SD = 0.07$ ). As predicted by its strong requirement for XRCC1 interaction, Polβ foci formation depends on its ability to bind XRCC1 (abrogated in copGFP-tagged Polβ(TM) and Polβ(TM/DM) mutants; Fig. 4E and [Supplementary Fig. S4C–E](#)).

While there is a small but discernable fraction of Polβ foci that colocalizes with phosphorylated H2AX foci in irradiated cells (Fig. 4F), Polβ foci are not associated with radiation-induced DSB repair markers such as 53BP1 (Fig. 4G and H), thereby largely excluding significant involvement in DSB repair processes. Importantly, TRIP12 promotes Polβ accumulation and foci formation, since TRIP12 depletion lowers baseline foci levels in untreated cells and abrogates Polβ foci induction by irradiation (Fig. 4I–K). TRIP12 depletion

affects the formation of large and persistent Polβ foci most profoundly, which appear to be characteristic of radiation exposure (Fig. 4J and K, and [Supplementary Fig. S4F](#)). In comparison, cisplatin treatment solely induces small Polβ foci that are, however, equally induced in TRIP12-shRNA expressing cells, indicating a lack of dependence on TRIP12 ([Supplementary Fig. S4G](#) and H). Notably, and consistent with its role in Polβ degradation, cytoplasmic levels of copGFP-Polβ were suppressed at 5 and 24 h after radiation (Fig. 4A) but not in cells expressing TRIP12 shRNA (Figs. 4I and J), further indicating radiation-induced TRIP12 activation that also facilitates cytoplasmic Polβ degradation as described above (Fig. 2D and [Supplementary Fig. S2F](#)).

TRIP12's role in Polβ recruitment after radiation is surprising when considering its previously reported DDR suppressive function [21] and suggests precedence for BER over DSB repair. The orchestration of repair protein engagement is indeed particularly challenging at complex DNA lesion sites that are typical of radiation exposure [48]. Risks due to a lack of repair coordination are two-fold: strand incision during repair can cause DSBs at counter-posing BER lesions, while base lesions can also hamper DSB repair. Thus, BER and DSB repair processes need to be tightly regulated both locally and temporally. Complex radiation-induced lesions with extensive BER lesions may therefore require a ruling in favor of BER (and before DSB repair) for optimal repair [49]. This led us to propose a DDR controller role for TRIP12 that ultimately prioritizes BER (through the ubiquitylation of Polβ) over DSB repair in the competition for access to complex lesions that may require both DNA repair processes.

### Role of Polβ levels in radiation response

Interference in the herein postulated DDR regulatory role could evoke a survival detriment. However, despite a large impact on the nuclear engagement of Polβ, TRIP12 depletion did not affect cellular survival (Fig. 3E–G). Radiation-induced complex lesion sites require highly balanced and coordinated BER/SSBR processes to prevent DSB formation from opposing lesion incisions [50]. While impacting Polβ recruitment after radiation, as shown here, TRIP12 depletion, however, also alleviates constraints on DSB signaling, which in turn facilitates compensatory DSB repair for cellular survival. In line with this, Lukas and colleagues found that depletion of TRIP12 led to an increase in the levels of RNF168 and promoted ubiquitylation near DNA damage sites with little increase in survival after radiation, as compared to controls [21]. In line with these earlier findings, we find that survival after radiation is not affected by TRIP12

with myc-HECT, myc-HECT(C2007A), myc-TRIP12-SB, or myc-TRIP12 expressed in and isolated from LN428 cells. Boxes indicate the fractions analyzed (FR1–FR4). Immunoblot of FR4 (right) indicates that Polβ is ubiquitylated by full-length myc-TRIP12 or the HECT domain but not the substrate-binding domain or the HECT domain with the active site mutation (C2007A). (B) TRIP12-HECT-dependent ubiquitylation. Immunoblots as in panel (A), using FR3 and FR4 from the Ubi assay as indicated in panel (A) with myc-HECT (wild-type or C2007A mutant) after different incubation times. (C) TRIP12-dependent ubiquitylation of transgenic Polβ in cells. Ubiquitylation of Flag-tagged wild-type Polβ [Flag-Polβ(WT)], XRCC1-binding mutant Polβ(L301R/V303R/V306R) [Flag-Polβ(TM)], and of the ubiquitylation and XRCC1-binding mutant Polβ(L301R/V303R/V306R/K206A/K244A) [Flag-Polβ(TM/DM)] was determined by IP/IB following transfection of HA-ubiquitin and using two different shRNA (sh1 and sh5) to TRIP12. Flag-IP HA antibody blotted lanes show ubiquitylation of pulled down proteins of which the majority are Polβ and Polβ complex-associated proteins. These are compared to IP input (WCL extracts) and probed for expression of PCNA (input loading control), Polβ, and HA (Ub). (D) TRIP12 affects cellular Polβ levels. Shown are changes (fold increase) in Polβ isoform levels, as listed [Flag-Polβ(WT), Flag-Polβ(TM), or Flag-Polβ(TM/DM)], in TRIP12-depleted cells (by TRIP12-sh1 or sh5 knockdown) when compared to their respective control-shRNA (SCR) expressing LN428 cells. Bar graph depicts average control-shRNA (SCR) normalized Polβ isoform levels as determined by multiple immunoblots (representative IB in [Supplementary Fig. S2D](#)), each indicated by a dot, with  $SD$  and  $n = 3–4$ . Asterisks indicate statistically significant differences (\*\* $P < .01$ , \*\*\*\* $P < .0001$ ; ANOVA) to the corresponding control-shRNA results.



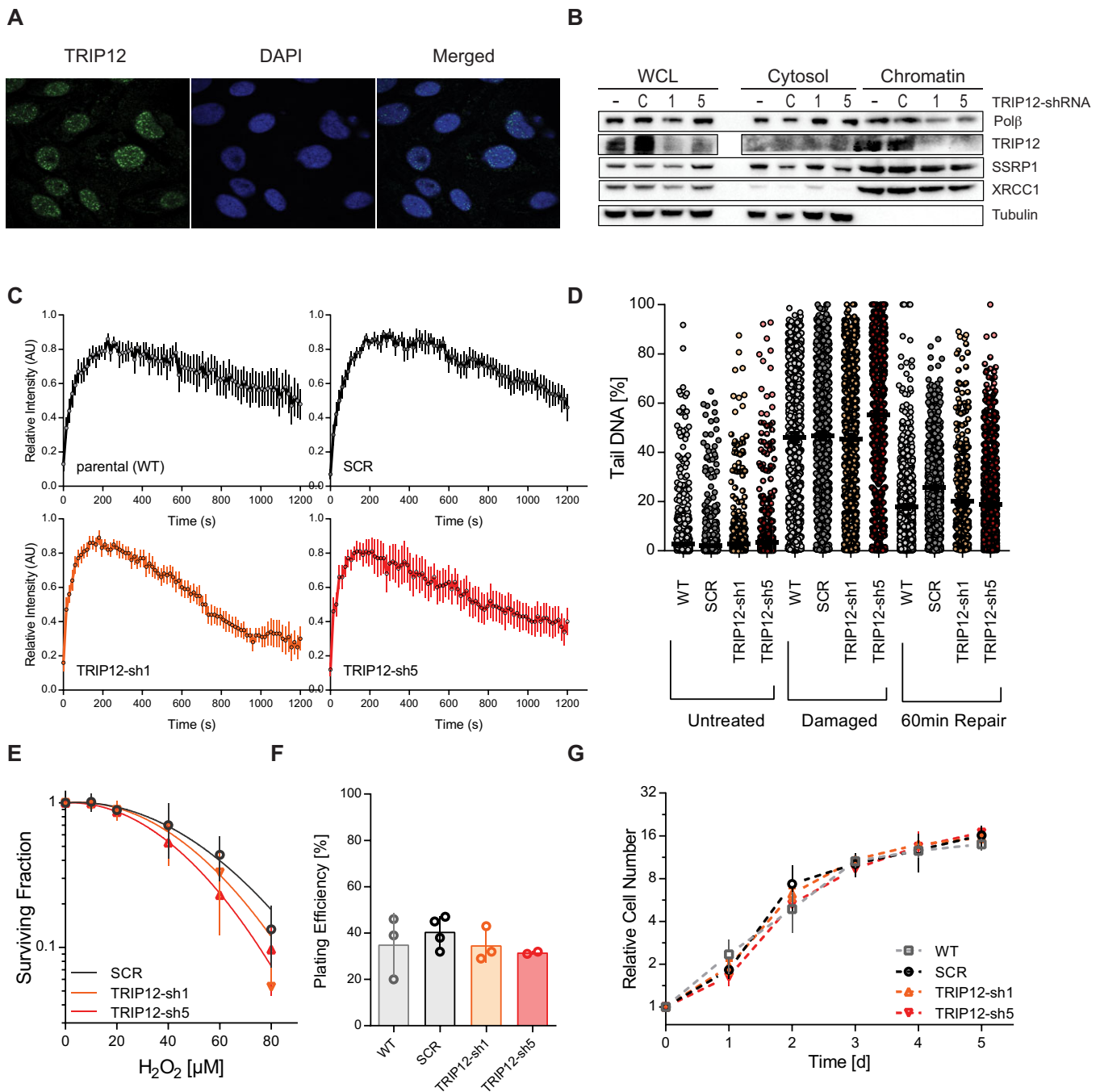


**Figure 3.** TRIP12-mediated Pol $\beta$  chromatin retention and BER function **(A)** Prominent nuclear localization of TRIP12. Confocal microscopy images showing nuclear (blue) localization of TRIP12 (green). **(B)** TRIP12-mediated Pol $\beta$  chromatin retention. Immunoblots show Pol $\beta$ , XRCC1, tubulin (cytosol fraction loading control), and SSRP1 (chromatin fraction loading control) levels in WCLs, the cytosolic or chromatin fraction in two different TRIP12-KD (knockdown) cell lines (TRIP12-sh1 and -sh5), scrambled controls (C), and the parental LN428 cell line (–) as indicated. **(C)** Laser damage induced focal recruitment of Pol $\beta$ , independent of TRIP12. Quantification of laser (405 nm)-induced local recruitment and retention of copGFP fused Pol $\beta$  (copGFP-Pol $\beta$ ) in TRIP12 knockdown (TRIP12-sh1 and -sh5) and control LN428 cell lines. Data are from  $n = 2$  independent experiments with each  $n = 10$  cells. **(D)** Effective oxidative damage repair in TRIP12-depleted cells. Oxidative damage and repair as determined by alkaline CometChip analyses (tail DNA in %) following a 30-min exposure to 250  $\mu M$   $H_2O_2$  (damaged) and at 60 min post-exposure (repair) in TRIP12-KD (TRIP12-sh1 and -sh5), scrambled (SCR), or parental (WT) control cell lines. **(E)** Cellular response to oxidative damage is not affected by the loss of TRIP12.  $H_2O_2$  sensitivity of TRIP12-depleted cell lines (TRIP12-sh1 and -sh5) is not significantly different from scrambled controls (SCR) as determined by clonogenic survival and curve fit comparisons or  $H_2O_2$  IC $_{50}$  determinations (ANOVA). Shown are the mean surviving fractions of three independent experiments  $\pm$  SD. **(F)** Depletion of TRIP12 does not affect cellular survival. No significant changes (ANOVA) were observed in the clonogenic survival of TRIP12-depleted cell lines (TRIP12-sh1 and -sh5), scrambled controls (SCR), and parental LN428 cells as determined by colony formation assays. The mean of three to four independent experiments, each indicated by dots with  $\pm$  SD, is shown. **(G)** Depletion of TRIP12 does not affect cell growth. TRIP12-depleted cell lines (TRIP12-sh1 and -sh5), LN428 parental cells (WT), and scrambled control (SCR) growth as determined by the MTT assay (mean and SD of  $n = 4$ ).

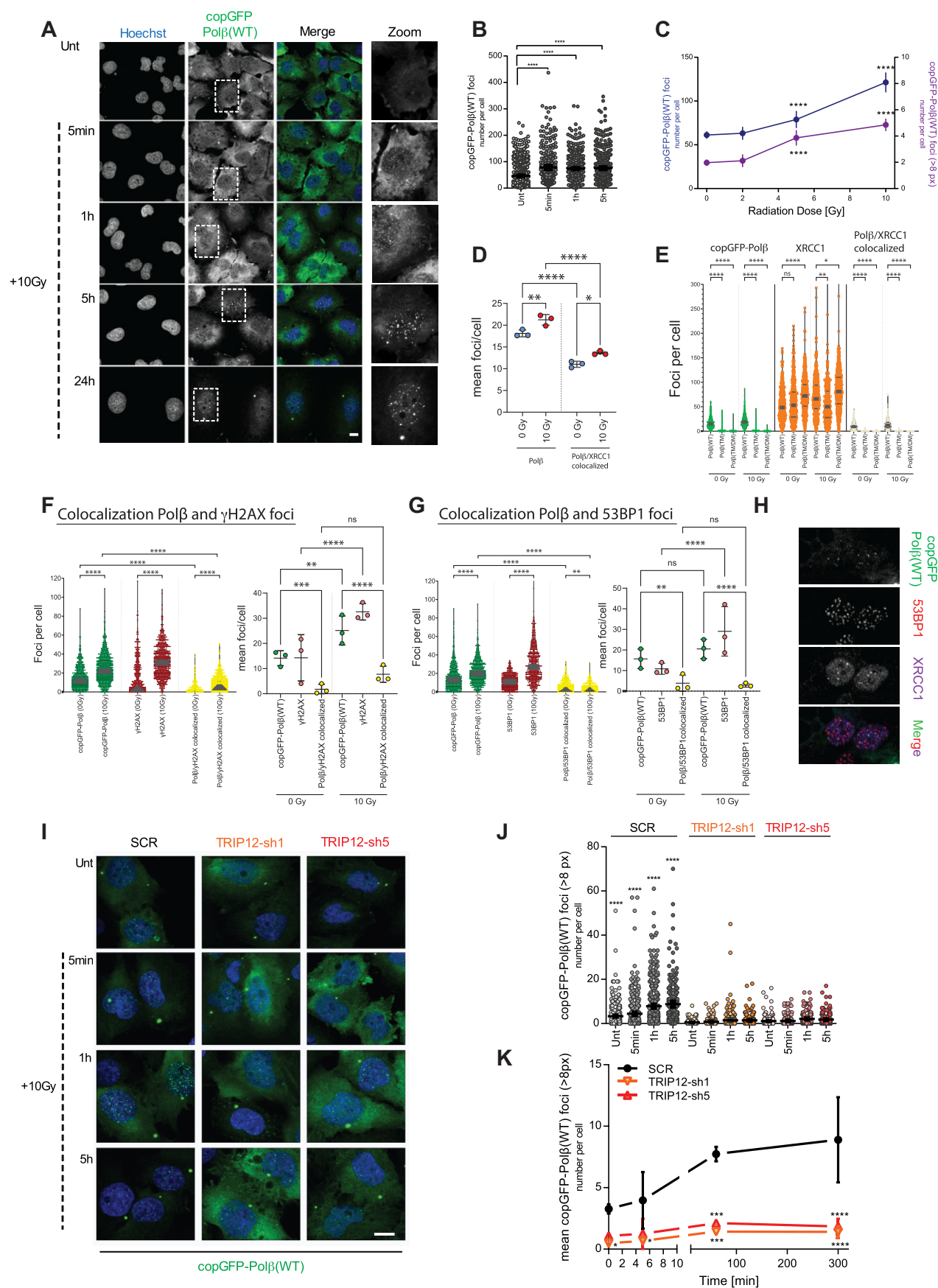


**Figure 4.** TRIP12 promotes radiation-induced Polβ foci formation. **(A)** Polβ foci formation by radiation. Representative images of copGFP-fused Polβ (copGFP-Polβ) foci in LN28 cells at different time points after radiation (10 Gy). **(B)** Characterization of radiation-induced Polβ foci over time. Dot plots

depletion (Fig. 5A). We therefore argued that, instead, excessive TRIP12-mediated shuttling of Pol $\beta$  due to Pol $\beta$  overabundance at supra-physiological levels (overexpression such as seen in some cancer types, developmental stages, and tissues) could expose prioritization of BER and the postulated concomitant suppression of DSB repair signaling. Supporting our proposition, we find that deregulation by Pol $\beta$  overexpression causes increased residual DSBs after radiation as determined by  $\gamma$ H2AX and 53BP1 foci (Fig. 5B). In line with these increased DSB levels, our data further show an increased sensitivity to radiation and reveal that the ultimate impact from Pol $\beta$  overexpression on the radiation response is as important as the loss of the SSBR/BER protein XRCC1 (Fig. 5C). Together, these data suggest that increased Pol $\beta$  levels can tip the balance toward persistent BER engagement attempts, thereby disrupting lesion repair leading to secondary and unresolved DSBs.

### TRIP12 and its Pol $\beta$ ubiquitylating activity affect radiation damage repair and response

These findings (Fig. 5) highlight the relevance of a finely tuned balance between BER and DSB repair protein levels in the maintenance of chromosomal integrity. TRIP12's role in Pol $\beta$  ubiquitylation and chromatin engagement (Figs 2 and 4), together with its reported DSB repair confinement function, points to TRIP12 as a likely candidate for such a regulatory role at the intersection of BER and DSB repair. Confirming TRIP12's governance of Pol $\beta$  and a ruling in favor of BER, TRIP12 depletion rescued cells from the Pol $\beta$  overexpression-induced phenotype that caused increased residual DSBs (Fig. 6A) and clonogenic cell death after radiation (Fig. 6B). Abrogating TRIP12 ubiquitylation sites on Pol $\beta$  [Pol $\beta$ (DM)] completely suppresses local Pol $\beta$  accumulation at earlier and later time points after radiation (Fig. 6C). Ubiquitylation of Pol $\beta$ , by TRIP12, is required for the interference in radiation damage repair, as

shown by the reduction of residual DSBs, as determined by  $\gamma$ H2AX and 53BP1 foci (Fig. 6D). Finally, abrogation of TRIP12 ubiquitylation also ultimately impedes the survival detriment caused by excess Pol $\beta$  and further confirms a functional link to TRIP12 (Fig. 6E). Thus, TRIP12 influences radiation response and controls Pol $\beta$  engagement through Pol $\beta$  ubiquitylation.

### TRIP12 at the intersection of DNA damage repair

Despite the observed decrease and deregulation of Pol $\beta$  in chromatin, TRIP12 depletion also causes extended RNF168-mediated chromatin signaling that leads to larger 53BP1 foci [21]. This process is supported by the E3 ubiquitin ligase UBR5, which, in conjunction with TRIP12, suppresses RNF168-facilitated 53BP1 chromatin loading [21]. Under-scoring TRIP12's unique and active role in Pol $\beta$  engagement and degradation, we, however, find that, in contrast to TRIP12, UBR5 loss (Supplementary Fig. S5A) does not alter cellular Pol $\beta$  levels or its chromatin loading (Supplementary Fig. S5B). Since UBR5 also suppresses RNF168, this therefore also excludes indirect effects caused by the excessive spreading of ubiquitylated chromatin.

Our findings suggest that TRIP12 can direct DNA repair activity at complex DSB lesion sites by (i) engaging Pol $\beta$  for BER at these sites and (ii) temporarily restraining chromatin ubiquitylation, which fosters DSB repair at these sites. In such a scenario, Pol $\beta$  will be recruited to lesion sites marked by  $\gamma$ H2AX, a process accompanied by a TRIP12-mediated delay in chromatin ubiquitylation, thus 53BP1 involvement. Testing this role in local repair segregation further, we conducted a series of colocalization analyses to characterize Pol $\beta$  foci further. Consistent with a radiation-induced recruitment to complex sites, we observed that a fraction of Pol $\beta$  foci colocalizes with  $\gamma$ H2AX foci (Fig. 4F). We find that recruitment of Pol $\beta$  to these  $\gamma$ H2AX foci is reduced in TRIP12-depleted cells (Fig. 7A–C and Supplementary Fig. S5C–F) and

show the distribution of copGFP-Pol $\beta$  foci in untreated cells (Unt) and in cells at 5 min, 1 h, or 5 h after 10 Gy ( $n = 3$  independent experiments with  $>50$  cells each). Mean foci/cell values per experiment and corresponding statistical evaluations are shown in Supplementary Fig. S4A and B. \*\*\*\* $P < .001$  in the Kruskal–Wallis test. (C) Pol $\beta$  foci formation is radiation dose dependent. Average copGFP-Pol $\beta$  foci counts per cell are shown of all foci (left Y axis and blue values) and of large foci ( $>8$  px, right Y axis with purple values) at 1 h after radiation. Data show mean and SD of pooled foci counts of two to three independent experiments and \*\*\*\* $P < .001$  indicate multiple comparisons adjusted to the respective unirradiated controls (ANOVA). (D) Pol $\beta$  foci colocalize with XRCC1. Changes in mean Pol $\beta$ (WT) foci/cell and Pol $\beta$ (WT)/XRCC1 colocalized foci of  $n = 3$  independent experiments are shown with \* $P < .05$ , \*\* $P < .01$ , \*\*\* $P < .001$ , and \*\*\*\* $P < .0001$  as determined by ANOVA. (E) Reduced Pol $\beta$  foci and XRCC1 colocalization of Pol $\beta$  isoforms devoid of XRCC1 binding [copGFP-Pol $\beta$ (TM) or copGFP-Pol $\beta$ (TM/DM)]. Violin plots show copGFP-Pol $\beta$  isoform foci [copGFP-Pol $\beta$ (WT), copGFP-Pol $\beta$ (TM), and copGFP-Pol $\beta$ (TM/DM)], XRCC1 foci in copGFP-Pol $\beta$ (WT), copGFP-Pol $\beta$ (TM), and copGFP-Pol $\beta$ (TM/DM) expressing cells, and copGFP-Pol $\beta$  isoform/XRCC1 colocalized foci distributions. Kruskal–Wallis test results are shown and interexperimental variations are shown in Supplementary Fig. S4C and D; representative images are shown in Supplementary Fig. S4E. (F) Majority of Pol $\beta$  foci do not colocalize with  $\gamma$ H2AX foci. Numbers of copGFP-Pol $\beta$ (WT),  $\gamma$ H2AX, and Pol $\beta$ (WT)/ $\gamma$ H2AX colocalized foci of individual cells (left) or mean foci/cell values per experiment (right) unirradiated and following 5 h after 10 Gy irradiation are shown; \* $P < .05$ , \*\* $P < .01$ , \*\*\* $P < .001$ , and \*\*\*\* $P < .0001$  as determined by Kruskal–Wallis (left) or ANOVA comparing the average of the means from three independent experiments (right). (G) Pol $\beta$  foci do not colocalize with 53BP1 foci. Numbers of copGFP-Pol $\beta$ (WT), 53BP1, and Pol $\beta$ (WT)/53BP1 colocalized foci of individual cells (left) or mean foci/cell values per experiment (right) unirradiated and following 10 Gy irradiation and 5-h repair are shown; \* $P < .05$ , \*\* $P < .01$ , \*\*\* $P < .001$ , and \*\*\*\* $P < .0001$  as determined by Kruskal–Wallis (left) or ANOVA comparing the average of the means from three independent experiments (right). (H) Representative images illustrating the quantified colocalization pattern of Pol $\beta$  and XRCC1 foci or lack thereof with 53BP1. (I) TRIP12-mediated Pol $\beta$  foci formation. Representative images of TRIP12-controlled Pol $\beta$  recruitment after radiation (10 Gy) in scrambled (SCR) control cells and TRIP12-depleted (TRIP12-sh1 and -sh5) cells. (J) Late and large Pol $\beta$  foci and Pol $\beta$  foci rich cells are particularly affected by TRIP12 depletion. Graph shows quantification of radiation-induced Pol $\beta$  [copGFP-Pol $\beta$ ] foci in scrambled (SCR) control and TRIP12-sh1 and -sh5 cells as indicated. Data show the number of large ( $>8$  px) Pol $\beta$  foci per cell from  $n = 3$  independent experiments with  $>50$  analyzed cells each; bars indicate means with SD. Asterisks mark multiple comparison adjusted  $P$ -values (\*\*\*\* $P < .0001$ ) in the Kruskal–Wallis test comparing the different cell line results at each time point to each other. (K) Robust abrogation of radiation-induced Pol $\beta$  foci by TRIP12 depletion. Quantification of radiation-induced Pol $\beta$  [copGFP-Pol $\beta$ ] foci in scrambled (SCR) control and TRIP12-sh1 and -sh5 cells as in panel (J). Graph demonstrates the interexperimental variation not visible in panel (J) and shows the average and SD of the means from  $n = 3$  independent experiments over time. Control SCR data used as reference; asterisks indicate significantly different mean foci numbers with \* $P < .05$ , \*\* $P < .01$ , and \*\*\*\* $P < .0001$  (ANOVA). ANOVA reports a significant interaction with  $P < 0.05$ . Radiation-induced foci are significantly different from untreated, only in the SCR for the 1 and 5 h data points with  $P < .001$  and  $P < .0001$ , respectively.



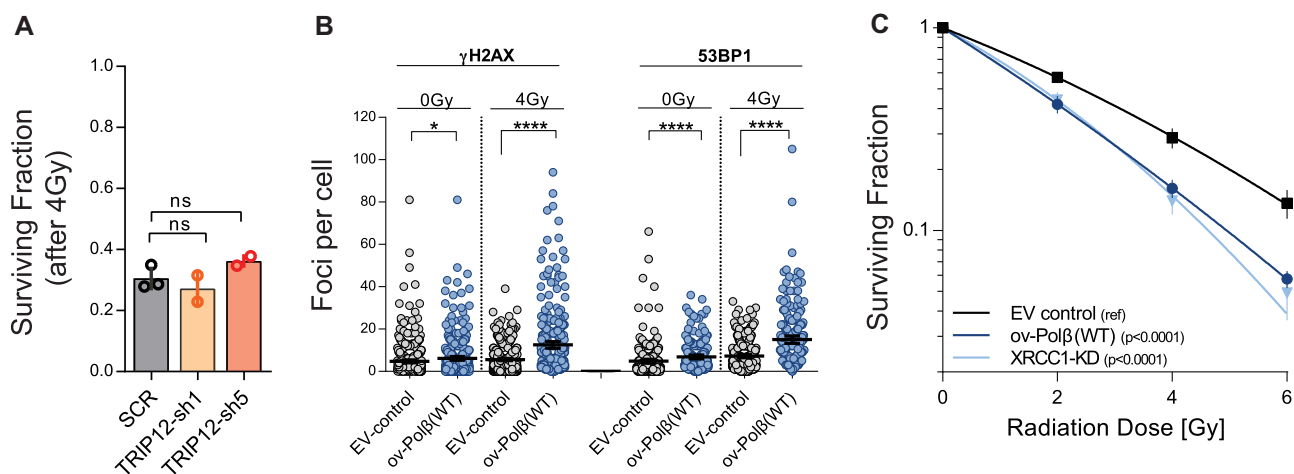


**Figure 5.** Repair interference by forced Polβ imbalance. **(A)** Radiation response is unaltered by TRIP12 depletion. TRIP12-depleted cells (TRIP12-sh1 and -sh5) were compared to scrambled (SCR) LN428 control cells. Clonogenic survival after 4 Gy with  $n = 2$ –3 independent experiments; errors are SD; and ns = non-significant ANOVA test results. **(B)** Polβ overexpression results in increased residual DSBs. Forced Polβ shuttling by excess Polβ results in increased residual γH2AX and 53BP1 foci per cell 24 h after radiation (4 Gy). Polβ overexpressing LN428 cells [ov-Polβ(WT)] were compared to empty vector controls (EV-control). Dot plots show foci per cell counts of  $n = 3$  independent experiments with minimal 50 cells each: \*  $P < .05$  and \*\*\*\*  $P < .0001$  (ANOVA). **(C)** Radiosensitization by deregulated Polβ. Cellular survival (clonogenicity as plating efficiency) and survival after radiation drops in Polβ overexpressing cells [ov-Polβ(WT)] to the same extent as in XRCC1-depleted (XRCC1-KD) cells. Bars and values show the mean and SD of the averages from three to seven independent experiments as indicated by the dots.  $P$ -values indicated in the radiation response curve graphs assess the likelihood of the data curve fits to be similar. Radiation response parameters (D37%) in the ov-Polβ(WT) and XRCC1-KD differ significantly from the reference (ref) EV-control cell line with  $P < .01$  and  $P < .01$  (ANOVA), respectively.

for the Polβ(TM/DM) variant that cannot be ubiquitinated by TRIP12 (Fig. 7D–F and [Supplementary Fig. S5F–H](#)). Consistent with the earlier finding of preferential TRIP12 binding to, and ubiquitylation of, the XRCC1-devoid BER complex binding, abrogation of XRCC1 binding does not affect recruitment to γH2AX foci (Fig. 7D–F and [Supplementary Fig. S5F–H](#)). We further observe that TRIP12 restrains nuclear colocalization of Polβ and 53BP1 (Fig. 7G and [Supplementary Fig. S5I–K](#)) in unirradiated conditions. Although low in numbers (Fig. 4G), this increased fraction of cells with colocalized Polβ and 53BP1 foci in TRIP12-shRNA expressing cells suggests that pathway segregation has been compromised at these lesions (Fig. 7G and [Supplementary Fig. S5L](#)). We also find a prominent, but largely TRIP12-independent, radiation-induced drop in the colocalization of Polβ and 53BP1 foci (Fig. 7G) that can be explained by the reduced engagement of Polβ at DSB sites in TRIP12-depleted cells. Together, these data illustrate how TRIP12 functions as a regulator of repair protein engagement at the intersection of BER and DSB repair pathways by revealing that TRIP12 and TRIP12 ubiquitylation sites support Polβ engagement at a fraction of γH2AX marked DSB sites (Fig. 7A–F) while at the same time reducing 53BP1 involvement as evidenced by reduced Polβ/53BP1 colocalization in its presence (Fig. 7G and [Supplementary Fig. S5L](#)).

In conclusion, our data indicate that TRIP12 functions as a DNA damage repair regulator at the intersection of BER and DSB repair processes by ubiquitylating Polβ at K206/K244 in an XRCC1 and BER complex type-dependent manner. TRIP12 facilitates chromatin association of Polβ, promoting radiation-induced engagement to γH2AX marked foci, while also restraining chromatin ubiquitylation. This has the impact of temporally reducing DSB repair pathway interference and ultimately regulating cellular Polβ levels, potentially guided through distinctive (mono- and poly-)ubiquitylation processes (graphically depicted in Fig. 7H).

## Discussion

The data presented here grant TRIP12 a central molecular role in DDR and repair pathway orchestration and reveal its important function in Polβ engagement and BER homeostasis. We show that TRIP12 binds to Polβ and through ubiquitylation controls cellular levels of Polβ and regulates Polβ chromatin retention upon DNA damage. The herein discovered role for TRIP12 at the nexus of DDR and repair pathways toward Polβ engagement and Polβ-directed repair results in the segregation of BER from RNF168/53BP1-initiated DSB repair pathways through its previously reported function in RNF168 and 53BP1 containment [21] (see the Graphical abstract). Such a “repair-controller” role is particularly important at complex DNA lesion sites to assure optimal DNA repair pathway choice and sequence to prevent damage aggravation.

## Importance of DNA repair pathway orchestration

The vital importance of genome maintenance is underscored by the evolution of multiple genome repair mechanisms, each of which function on a specific type or class of damaged DNA [51]. Of these, the BER pathway plays a critical role in repairing the most abundant type of DNA lesions. DNA SSBs, nicks, and replication-blocking base lesions are the most critical among BER targets. If not repaired, they can give rise to DSBs that ultimately require repair by NHEJ or HR, depending on the context in which they arise. Ionizing radiation induces clustered DNA lesions with base damage, SSBs, and DSBs in close proximity to each other. They are therefore particularly challenging lesions to repair that require a well-coordinated BER-mediated strand incision sequence to prevent DSB formation [50, 52–55]. Since the complexity of this type of damage also hampers DSB repair if located close to or at DSBs, cellular mechanisms that direct the order of repair activities are critical for genome maintenance, suggesting



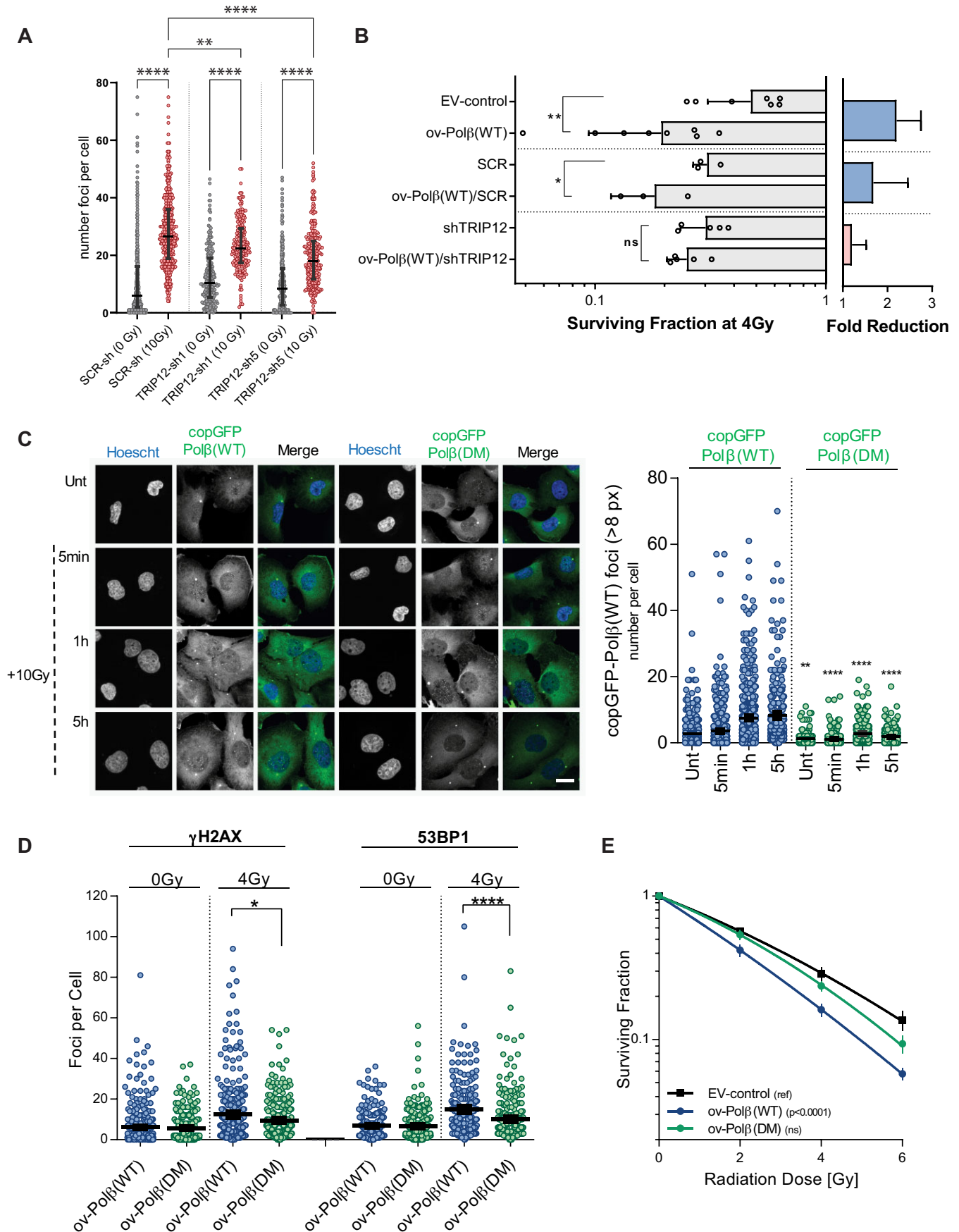


**Figure 6.** TRIP12 influences radiation response through Pol $\beta$  ubiquitylation. **(A)** TRIP12 depletion reduces Pol $\beta$  overexpression-induced DSB formation after radiation. Numbers of  $\gamma$ H2AX foci per cell in copGFP-Pol $\beta$  overexpressing scrambled (SCR) control cells and TRIP12-depleted (TRIP12-sh1 and

that a prioritization of BER and the prevention of, in this case, futile DSB repair may be of vital importance to cells. Indeed, functional or physical crosstalk among DNA repair pathways is emerging as an essential aspect of the overall cellular response to DNA damage [15, 56–58]. This has been extensively described for repair pathways dealing with DSBs or crosslinks. However, the BER/DSB repair pathway orchestration postulated here has not yet been defined and links repair pathways across classes that are intrinsically very different. Our study portrays TRIP12 at the nexus of these main cellular repair activities (Fig. 7H; see the Graphical abstract).

The recently discovered binding of TRIP12 to PARP1, another important BER and SSB member, and its ability to regulate steady-state levels of PARP1 through (poly-)ubiquitylation, is in line with our model and our proposed repair coordination and control function [22]. Like the notion elucidated by us, the authors suggested that the relevance of this process lies in the prevention of supra-physiological PARP1 accumulation and activity. Indeed, in our study we were able to demonstrate the detrimental effects of supra-physiological Pol $\beta$  levels in our overexpression models and thus a role for TRIP12 in genomic stability.

### TRIP12's role in radiation damage repair

Our study uncovers a new cellular function of TRIP12 and identifies TRIP12 as a key regulator of BER repair activity through Pol $\beta$  engagement. Here, we show ionizing radiation-induced Pol $\beta$  foci formation and reveal that TRIP12 is essential for Pol $\beta$  engagement in the cellular response to radiation. Notably, TRIP12 requirement is also evident for those foci that arise under unchallenged conditions; however, Pol $\beta$  recruitment at lesions induced by laser irradiation intensities that do not cause DSBs or clustered lesions is not affected (Fig. 3C and Supplementary Fig. S3C), nor is the small induction of Pol $\beta$  foci by cisplatin, which also does not directly induce DSBs (Supplementary Fig. S4E and F). In contrast, but consistent with the herein proposed role of TRIP12 at the nexus of BER and DSB repair, TRIP12 is involved in foci induction after radiation. This functional link between TRIP12 and Pol $\beta$  is further strengthened by the inability of Pol $\beta$  mutants, devoid of TRIP12-mediated ubiquitylation (Fig. 2C and Supplementary Fig. S2B), to form Pol $\beta$  foci at background levels or after radiation, consistent with the TRIP12 knock-down data (Figs 4I–K and 6C). More so, we were able to confirm TRIP12's involvement in the nuclear activities of Pol $\beta$  by showing the rescue in DSB induction and the radiation sur-

vival detriment from Pol $\beta$  deregulation in TRIP12 ubiquitylation mutants and TRIP12-depleted cells (Fig. 6).

Initially, and despite the drastic reduction in Pol $\beta$  engagement, we were not able to identify cellular defects in TRIP12-deficient cells (Fig. 3 and Supplementary Fig. S3C and D) except for the elevated expression of RNF168 (Supplementary Fig. S3B). This lack of an impact on cellular survival or radiation sensitivity is not surprising as Pol $\beta$ -deficient cells have been reported to survive well in culture and show similar radiation survival as their wild-type counterparts [29, 59–62]. Indeed, a role for Pol $\beta$  in the cellular radiation response could only be identified after isolating replicating cells or applying dominant-negative transgenes that interfered in BER [59–62]. Overall, this observation is also consistent with earlier reports from Gudjonsson *et al.* [21], who did not report a deficit in cellular survival upon depletion of TRIP12, and from Kajiro *et al.* who describe a minor impact of TRIP12-HECT domain mutations on the proliferation of ES cells [63]. The lack of radiation sensitivity is also in line with the notion that TRIP12 deficiency unlocks DSB repair capacity [21, 64], which may rescue any potential cellular impact from DSBs caused by the loss of Pol $\beta$ -mediated repair [64–67].

### TRIP12's role in Pol $\beta$ homeostasis

Pol $\beta$  and XRCC1 are important elements in BER; their equilibrium appears to be critical for BER function [3, 36, 37, 68]. Of these two, Pol $\beta$  provides both DNA polymerase and 5' dRP lyase activities essential to complete base lesion repair [7, 29, 69]. By performing colocalization experiments after radiation, we found that Pol $\beta$  resides at most XRCC1 sites (Fig. 4D, E, and H, and Supplementary Fig. S4D and E), underlining the relevance of XRCC1/Pol $\beta$  complex formation [37]. Our previous findings and reports from others revealed that both Pol $\beta$  and XRCC1 play common but also separate and independent roles in DNA metabolism and repair [3, 70]. We previously discovered that the composition of BER protein complexes depends on the cell cycle and DNA damage type [3] and observed a shift toward HSP90-bound XRCC1, devoid of Pol $\beta$ . Since Pol $\beta$  levels remained constant, it suggested a considerable pool of a Pol $\beta$ -centric BER complex (herein termed Complex B) and a mechanism to mediate this shift that depended on Pol $\beta$  as it was absent in Pol $\beta$  knockout cells [3]. The considerable increase in Pol $\beta$  degradation, when unable to bind to XRCC1 [Pol $\beta$ (TM)], further substantiated the suspicion of a complex-dependent and Pol $\beta$ -specific E3 ubiquitin ligase activity in these previous studies [3, 36]. Herein, we

-sh5) cells are shown, unirradiated and 5 h following 10 Gy irradiation as indicated; \* $P < .05$ , \*\* $P < .01$ , \*\*\* $P < .001$ , and \*\*\*\* $P < .0001$  as determined by Kruskal–Wallis. (B) TRIP12 depletion rescues cells from Pol $\beta$  overexpression-mediated radiosensitization. Reduced survival after radiation by the overexpression of wild-type Pol $\beta$  [ov-Pol $\beta$ (WT)] (Fig. 5C) in empty vector (EV-control) or SCR (scrambled shRNA) controls is rescued by TRIP12 depletion (TRIP12-sh1 and -sh5). The graph shows the average clonogenic survival after 4 Gy and the SD in  $n = 3$ –7 independent experiments as indicated by the dots. The Pol $\beta$  overexpression-induced fold reduction in radiation survival is indicated to the right; \* $P < .05$  and \*\* $P < .01$  (ANOVA). (C) Mutation of the TRIP12 ubiquitylation sites (K206A/K244A) on Pol $\beta$  abrogates Pol $\beta$  focal accumulation after radiation. Representative images and quantification of radiation-induced Pol $\beta$  [copGFP-Pol $\beta$ (WT)] and ubiquitylation mutant Pol $\beta$ (DM) [copGFP-Pol $\beta$ (DM)] foci. The graph (right) shows the number of large (>8 px) mutant or wild-type Pol $\beta$  foci per cell at different time points after radiation from  $n = 3$  independent experiments with means and SD; \* $P < .05$  and \*\* $P < .01$  (ANOVA). (D) Abrogation of TRIP12 ubiquitylation sites on Pol $\beta$  reduces DSB induction. Residual  $\gamma$ H2AX and 53BP1 foci at 24 h are shown in untreated cells and 4-Gy irradiated cells that overexpress wild-type Pol $\beta$  [ov-Pol $\beta$ (WT)] or the Pol $\beta$  K206A/K244A ubiquitylation mutant [ov-Pol $\beta$ (DM)]; \* $P < .05$  and \*\* $P < .01$  (ANOVA). (E) TRIP12 ubiquitylation site mutation in Pol $\beta$  rescues cells from Pol $\beta$  overexpression-mediated radiosensitivity. Pol $\beta$ (WT) overexpressing cells are compared to Pol $\beta$ (DM) overexpressing and empty vector (EV-control) LN428 control cells. Surviving fractions after 2, 4, and 6 Gy are shown with data points indicating the averages with SEM of the mean values from  $n = 3$ –8 independent experiments.  $P$ -values indicated in the legend of the radiation response curve graph assess the likelihood of the data curve fits to be similar to the reference EV-control response curve. Radiation response parameters (D37%) in the ov-Pol $\beta$ (DM) cell line are not significantly different from the EV-control (ns), compared to the ov-Pol $\beta$ (WT) that differ significantly from the reference (ref) EV-control cell line with  $P < .01$  (ANOVA).

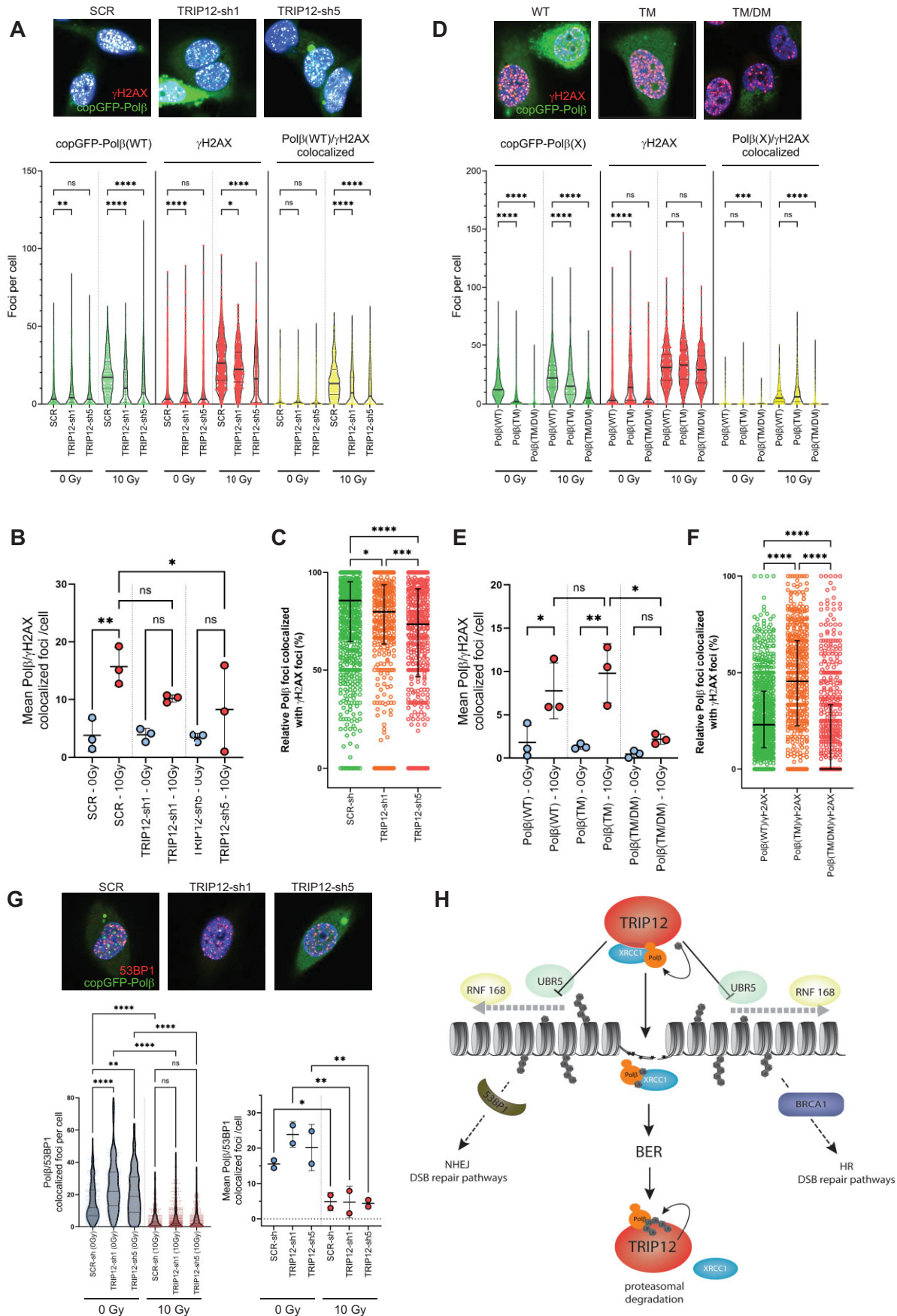


**Figure 7.** TRIP12's controller function in DNA repair pathway engagement and choice. **(A)** TRIP12's role in Polβ engagement to γH2AX marked chromatin. Representative images show decreased colocalization (white) of Polβ (green) and γH2AX (red) in TRIP12-depleted cells. Violin dot plots



identified, via label-free dMS, TRIP12 as this complex-dependent E3 ubiquitin ligase. Pol $\beta$  is a substrate for TRIP12 both *in vitro* and in cells, and the interaction is between the SB domain (TRIP12-SB) of TRIP12 and the C-terminal domain of Pol $\beta$ . At this stage, we are not able to fully disentangle whether TRIP12 has a lessened influence on XRCC1-bound Pol $\beta$  and can contribute to a shift toward the XRCC1-free complex or whether directed by other mechanisms, this state enables TRIP12 interference, thus ubiquitylation and Pol $\beta$  foci formation. We did, however, observe a reduction in cytoplasmic Pol $\beta$  levels after radiation at late time points (Fig. 4A). Together with the expected overall increase in levels (due to the lack of degradation processes), this reduction was absent in TRIP12 knockdown cells (Fig. 4I). TRIP12's contribution to Pol $\beta$  elimination supports a role in re-establishing baseline values after successful repair, further highlighting the importance of well-balanced Pol $\beta$  levels. This may address the observed paradoxical role of TRIP12 in promoting Pol $\beta$  engagement in the nucleus in response to damage on one hand while also facilitating Pol $\beta$  degradation after the insult on the other [26, 71–76].

### Pol $\beta$ in TRIP12-regulated processes

Little is known about the cellular role of TRIP12, a HECT-type E3 ubiquitin ligase. ARF and App-BP1 have been reported to be among TRIP12 ubiquitylation targets, implicating TRIP12 in ubiquitin fusion degradation, neddylation, or the ARF-regulated p53 response [44, 77–79]. The first indications for its involvement in DNA repair processes came from data revealing a role in 53BP1 foci formation [21] and a link to the DDR through USP7 ubiquitylation [27]. Gudjonsson *et al.* also showed that TRIP12 acts as a suppressor of RNF168, reducing the accumulation of “Lys-63”-linked histones H2A and H2AX at DNA damage sites and revealed its partnership with UBR5 [21]. TRIP12 thereby acts as a guard against the excessive spreading of ubiquitylated chromatin at damaged chromosomes that are thought to facilitate the accumulation of repair proteins [21, 80]. Here, we were able to juxtapose TRIP12's restraining function of DSB repair with a repair-promoting activity by direct engagement of Pol $\beta$ , an essential

BER factor. The lack of colocalization of Pol $\beta$  with 53BP1 (Figs 4G and 7G, and [Supplementary Fig. S5K](#)) supports this link. Interestingly, we find that in contrast to TRIP12, its partner UBR5 does not affect the chromatin association of Pol $\beta$  ([Supplementary Fig. S5A and B](#)).

Indeed, BER may not require extensive chromatin rearrangement as indicated by fast recruitment kinetics in heterochromatic regions [81]. The repair of radiation-induced clustered lesions will benefit from early BER engagement and restricted chromatin rearrangement to prevent DSB formation or DSB repair attempts at lesion sites. In this context, Eccles *et al.* showed the importance of, the then unknown, nuclear factors in the sequence of events at such sites [82]. At this point, we are not able to discern whether the late and large Pol $\beta$  foci are a consequence of retention due to continued loading attempts by TRIP12 from incomplete repair or the engagement in late, secondary DSB repair processes. The impact of TRIP12 deficiency in the early and small foci, however, confirms a loading role for most of these foci. This is also consistent with a damage-type specific role of TRIP12 as shown by the lack of such a response modulation after H<sub>2</sub>O<sub>2</sub> or cisplatin. Since radiation induces a large amount of both Pol $\beta$  and 53BP1 foci, the drop in Pol $\beta$ /53BP1 colocalization reveals an active segregation process early after radiation that is, in part, TRIP12-dependent (Fig. 7G and [Supplementary Fig. S5K and L](#)). Not all DSBs are highly complex, i.e. coinciding with multiple BER targeted lesions. Indeed, we observed that only few  $\gamma$ H2AX marked foci, and substantially less 53BP1 foci, contain Pol $\beta$ . Different staining conditions and imaging settings impair comparisons across the different colocalization datasets; yet, it appears that, 5 h after irradiation, most Pol $\beta$  foci can be found colocalized with  $\gamma$ H2AX, a process dependent on TRIP12 or TRIP12 ubiquitylation sites (Fig. 7C and F). Since TRIP12 depletion affects radiation-induced engagement with  $\gamma$ H2AX chromatin, it is difficult to assess the impact of TRIP12 depletion on pathway segregation (thus test for increased Pol $\beta$ /53BP1 colocalization). Yet, we observe significantly increased foci colocalization events in unirradiated cells (Fig. 7G) and increased Mander's overlap coefficient values before and after radiation in time course experiments in TRIP12-depleted cells ([Supplementary Fig. S5L](#)),

show the distribution of copGFP-Pol $\beta$ ,  $\gamma$ H2AX, and Pol $\beta$ / $\gamma$ H2AX colocalized foci in scrambled (SCR) shRNA-expressing or TRIP12-depleted (TRIP12-sh1 and -sh5) unirradiated control (0 Gy) cells and 5 h after 10 Gy irradiation ( $n = 3$  independent experiments with  $>100$  cells each); \* $P < .05$ , \*\* $P < .01$ , \*\*\* $P < .001$ , and \*\*\*\* $P < .0001$  as determined by Kruskal–Wallis. (B) Mean colocalized foci/cell values per experiment, pooled in panel (A), and corresponding statistical evaluations (\* $P < .05$  and \*\* $P < .01$  from ANOVA) are shown. (C) The relative numbers of Pol $\beta$  colocalized with  $\gamma$ H2AX (on a cell-by-cell basis) in irradiated cells are shown with medians and interquartile ranges. (D) Role of TRIP12 ubiquitylation site in Pol $\beta$  engagement to  $\gamma$ H2AX marked chromatin. Representative images show decreased colocalization (white) of the TRIP12 ubiquitylation-mutated copGFP-Pol $\beta$ (TM/DM) isoform (green) and  $\gamma$ H2AX (red). Violin dot plots show the distribution of the copGFP-Pol $\beta$  isoforms [copGFP-Pol $\beta$ (WT), copGFP-Pol $\beta$ (TM), copGFP-Pol $\beta$ (TM/DM)], as indicated,  $\gamma$ H2AX, and Pol $\beta$ / $\gamma$ H2AX colocalized foci in control (0 Gy) cells and 5 h after 10 Gy irradiation ( $n = 3$  independent experiments with  $>100$  cells each); \* $P < .05$ , \*\* $P < .01$ , \*\*\* $P < .001$ , and \*\*\*\* $P < .0001$  as determined by the Kruskal–Wallis test. (E) Mean foci/cell values per experiment and corresponding statistical evaluations (\* $P < .05$  from ANOVA) are shown. (F) The relative numbers of Pol $\beta$  [copGFP-Pol $\beta$ (WT), copGFP-Pol $\beta$ (TM), or copGFP-Pol $\beta$ (TM/DM)] colocalized with  $\gamma$ H2AX (on a cell-by-cell basis) are shown with medians and interquartile ranges. (G) Influence of TRIP12 on colocalization of Pol $\beta$  with 53BP1. CopGFP-Pol $\beta$  and 53BP1 foci colocalization in control (SCR) and TRIP12 knockdown cells (sh1 and sh5) 5 h after 10 Gy irradiation are shown and compared to unirradiated controls (0 Gy) in violin dot plots illustrating changes in median and distribution (left graph) and as mean foci/cell values from two independent experiments with at least  $n = 100$  cells each (right graph; see [Supplementary Fig. S5](#) for additional data). Asterisks mark  $P$ -values (Kruskal–Wallis test, \*\*\*\* $P < .0001$ , \*\* $P < .01$ ) assessing the impact of TRIP12 depletion and radiation on these cells. (H) TRIP12 in the governance of repair pathway choice. A graphic is shown that illustrates the current working model of TRIP12 involvement in BER. TRIP12-mediated prevention of the RNF168 promoted histone ubiquitylation extension surrounding DNA lesions restrains DSB signaling in favor of Pol $\beta$ . Enabled by its ubiquitylation activity on Pol $\beta$ , TRIP12 exerts its repair traffic control function by assisting BER and deviating DSB repair at the same time. Complex damage sites with clustered lesions can cause DSBs if not repaired appropriately and DSB repair attempts at DSBs residing in such regions may fail due to the presence of such BER-targeted lesions, since they prevent synthesis and nuclease activities. A cellular control mechanism that channels repair proteins to yield the right of way to BER may be therefore relevant in these cases. A two-step activity can be proposed in which TRIP12 engages Pol $\beta$  at nuclear damage sites but also initiates BER complex disassembly, freeing Pol $\beta$  from XRCC1 for distinct repair activities and thereafter destines Pol $\beta$  for proteasome degradation upon repair completion.



suggesting that the segregation is compromised. It should be noted that in order to detect any potential Pol $\beta$ /53BP1 associations in this low colocalization context (Fig. 4G and H), these analyses (Fig. 7G) were conducted at different settings that comprise very small foci or simply protein localization (Supplementary Fig. S5L).

Combined with TRIP12's Pol $\beta$ -regulatory activity shown here, BER engagement and 53BP1 exclusion further support our hypothesis that assigns TRIP12 a role in the sequence of repair activities. We postulate that the provenance of TRIP12 ubiquitylation activity on Pol $\beta$  is to enable a timely order of repair by ranking BER activities over those from the DSB repair machinery through an active role in Pol $\beta$  chromatin association and the concomitant regulation of initial DDR modulators.

### Dual function of TRIP12: repair pathway coordination and protein homeostasis

Here, we observed a clear role for TRIP12 in the governance of Pol $\beta$  chromatin loading as well as cellular Pol $\beta$  levels. Ubiquitylation plays a role in protein stability for many DNA repair proteins, whereas non-proteolytic functions of ubiquitin (either mono-ubiquitin or poly-ubiquitin) are essential for signaling in DNA replication and DNA repair [83, 84]. As part of our dynamic BER model [3], we deduced that ubiquitylation of Pol $\beta$  may facilitate repair pathway choice similar to ubiquitylation in DSB repair processes [83, 85]. The poly-ubiquitin mark can play a signaling role as well as facilitate proteolysis [86, 87]. Herein, we suggest that Pol $\beta$  is regulated by TRIP12-mediated ubiquitylation, possibly assisted by additional E3 ubiquitin ligases. We observe TRIP12-dependent generation of both (mono- and poly-)ubiquitylated species of Pol $\beta$  in the *in vitro* "on-bead" assay (Fig. 2A and B). This is in line with a role for ubiquitylation in both signaling and protein homeostasis that may depend on ubiquitin chain types. Future analyses will be essential to differentiate what role, if any, is ascribed to (mono- and poly-)ubiquitylation. Consistent with a role for Pol $\beta$  ubiquitylation in repair and signaling, here we show that TRIP12 and the ubiquitylation of Pol $\beta$  at K206/K244 are essential for Pol $\beta$  chromatin association and foci induction and in the maintenance of cellular Pol $\beta$  levels.

In conclusion, we propose that TRIP12 functions as a "repair-sequence-controller," through ubiquitylation, facilitating pathway crosstalk across significantly different repair processes that require a different extent of chromatin modulation. By coordinating Pol $\beta$  and DSB repair engagement, TRIP12 may ultimately prevent the conversion of base lesions and single-strand breaks to cytotoxic and genotoxic DSBs.

### Acknowledgements

We thank S.H. Wilson (NIEHS/NIH) for the gift of recombinant human DNA polymerase  $\beta$  used for some of this project. We also thank T. Sixma for carefully reading the manuscript and offering constructive comments.

**Author contributions:** Burcu Inanc (Data curation [equal], Investigation [equal], Methodology [equal], Writing—original draft [equal]), Qingming Fang (Data curation [equal], Investigation [equal], Methodology [equal], Writing—original draft [equal]), Wynand Paul Roos (Data curation [supporting], Investigation [supporting], Methodology [supporting]),

Xuemei Zeng (Investigation [supporting], Data curation [supporting]), Joel F. Andrews (Methodology [supporting]), Jennifer Clark (Investigation [supporting]), Jianfeng Li (Investigation [supporting]), Nupur B. Dey (Investigation [supporting]), Md Ibrahim (Investigation [supporting]), Peter Sykora (Investigation [supporting]), Zhongxun Yu (Investigation [supporting]), Charlotte R. Pearson (Investigation [supporting]), Andrea Braganza (Investigation [supporting]), Marcel Verheij (Funding acquisition [supporting], Resources [supporting]), Jos Jonkers (Funding acquisition [supporting], Resources [supporting]), Nathan A. Yates (Conceptualization [supporting], Data curation [supporting], Funding acquisition [supporting], Methodology [supporting], Resources [supporting]), Conchita Vens (Conceptualization [equal], Data curation [equal], Formal analysis [equal], Funding acquisition [equal], Investigation [equal], Methodology [equal], Project administration [equal], Resources [equal], Supervision [equal], Writing—original draft [equal], Writing—review & editing [equal]), and Robert W. Sobol (Conceptualization [equal], Data curation [equal], Formal analysis [equal], Funding acquisition [equal], Investigation [equal], Methodology [equal], Project administration [equal], Resources [equal], Supervision [equal], Writing—original draft [equal], Writing—review & editing [equal]).

### Supplementary data

Supplementary data is available at NAR online.

### Conflict of interest

None declared.

### Funding

This study was supported by funds from the National Institutes of Health (CA148629, ES014811, ES029518, and CA238061 to R.W.S.), the Dutch Cancer Society KWF (NKI-2010-4877 to C.V.), and CRUK (CRUK-RADNET Glasgow to C.V.). This study used the Hillman Cancer Center Proteomics Facility that is supported in part by award P30CA047904 from NIH. Support for the USA Mitchell Cancer Institute (MCI) Cellular and Biomolecular Imaging Facility and the USA MCI Flow Cytometry Facility was provided by funds from the Abraham A. Mitchell Distinguished Investigator award and USA MCI Core Facility funds. Support for the NKI microscopy facility was provided by operating funds of the Netherlands Cancer Institute (NKI). Support was also provided by the Legoretta Cancer Center Endowment Fund (to R.W.S.). The purchase and maintenance of the Nikon Ti2-E inverted confocal microscope with Ax-R in our lab at Brown University was provided by generous support from the Dr. Robert Browning Foundation. Funding to pay the Open Access publication charges for this article was provided by NIH grant ES029518 & the Legoretta Cancer Center Endowment Fund.

### Data availability

All data is available upon request. Mass spectrometry proteomics data have been deposited in the MassIVE repository, under accession code MSV000094615.

## References

- Hustedt N, Durocher D. The control of DNA repair by the cell cycle. *Nat Cell Biol* 2017;19:1–9. <https://doi.org/10.1038/ncb3452>
- Clouaire T, Legube G. DNA double strand break repair pathway choice: a chromatin based decision? *Nucleus* 2015;6:107–13.
- Fang Q, Inanc B, Schamus S *et al.* HSP90 regulates DNA repair via the interaction between XRCC1 and DNA polymerase  $\beta$ . *Nat Commun* 2014;5:5513. <https://doi.org/10.1038/ncomms6513>
- Kakarougkas A, Jeggo PA. DNA DSB repair pathway choice: an orchestrated handover mechanism. *Br J Radiol* 2014;87:20130685. <https://doi.org/10.1259/bjr.20130685>
- Kratz A, Kim M, Kelly MR *et al.* A multi-scale map of protein assemblies in the DNA damage response. *Cell Syst* 2023;14:447–63.e448. <https://doi.org/10.1016/j.cels.2023.04.007>
- Svilar D, Vens C, Sobol RW. Quantitative, real-time analysis of base excision repair activity in cell lysates utilizing lesion-specific molecular beacons. *J Vis Exp* 2012;6:e4168.
- Almeida KH, Sobol RW. A unified view of base excision repair: lesion-dependent protein complexes regulated by post-translational modification. *DNA Repair (Amst)* 2007;6:695–711. <https://doi.org/10.1016/j.dnarep.2007.01.009>
- Breimer LH, Lindahl T. Thymine lesions produced by ionizing radiation in double-stranded DNA. *Biochemistry* 1985;24:4018–22. <https://doi.org/10.1021/bi00336a032>
- Nackerdien Z, Olinski R, Dizdaroğlu M. DNA base damage in chromatin of gamma-irradiated cultured human cells. *Free Radic Res Commun* 1992;16:259–73. <https://doi.org/10.3109/10715769209049179>
- Della-Maria J, Zhou Y, Tsai MS *et al.* Human Mre11/human Rad50/Nbs1 and DNA ligase III $\alpha$ /XRCC1 protein complexes act together in an alternative nonhomologous end joining pathway. *J Biol Chem* 2011;286:33845–53. <https://doi.org/10.1074/jbc.M111.274159>
- Audebert M, Salles B, Calsou P. Involvement of poly(ADP-ribose) polymerase-1 and XRCC1/DNA ligase III in an alternative route for DNA double-strand breaks rejoining. *J Biol Chem* 2004;279:55117–26. <https://doi.org/10.1074/jbc.M404524200>
- Soni A, Siemann M, Grabos M *et al.* Requirement for Parp-1 and DNA ligases 1 or 3 but not of Xrcc1 in chromosomal translocation formation by backup end joining. *Nucleic Acids Res* 2014;42:6380–92. <https://doi.org/10.1093/nar/gku298>
- Citterio E. Fine-tuning the ubiquitin code at DNA double-strand breaks: deubiquitinating enzymes at work. *Front Genet* 2015;6:282. <https://doi.org/10.3389/fgene.2015.00282>
- Mattioli F, Vissers JH, van Dijk WJ *et al.* RNF168 ubiquitinates K13-15 on H2A/H2AX to drive DNA damage signaling. *Cell* 2012;150:1182–95. <https://doi.org/10.1016/j.cell.2012.08.005>
- Panier S, Durocher D. Push back to respond better: regulatory inhibition of the DNA double-strand break response. *Nat Rev Mol Cell Biol* 2013;14:661–72. <https://doi.org/10.1038/nrm3659>
- Uckelmann M, Sixma TK. Histone ubiquitination in the DNA damage response. *DNA Repair (Amst)* 2017;56:92–101. <https://doi.org/10.1016/j.dnarep.2017.06.011>
- Chroma K, Mistrik M, Moudry P *et al.* Tumors overexpressing RNF168 show altered DNA repair and responses to genotoxic treatments, genomic instability and resistance to proteotoxic stress. *Oncogene* 2017;36:2405–22. <https://doi.org/10.1038/ncr.2016.392>
- Bouwman P, Aly A, Escandell JM *et al.* 53BP1 loss rescues BRCA1 deficiency and is associated with triple-negative and BRCA-mutated breast cancers. *Nat Struct Mol Biol* 2010;17:688–95. <https://doi.org/10.1038/nsmb.1831>
- Zong D, Adam S, Wang Y *et al.* BRCA1 haploinsufficiency is masked by RNF168-mediated chromatin ubiquitylation. *Mol Cell* 2019;73:1267–81. <https://doi.org/10.1016/j.molcel.2018.12.010>
- Porro A, Sartori AA. Context matters: RNF168 connects with PALB2 to rewire homologous recombination in BRCA1 haploinsufficiency. *Mol Cell* 2019;73:1089–91. <https://doi.org/10.1016/j.molcel.2019.03.005>
- Gudjonsson T, Altmeyer M, Savic V *et al.* TRIP12 and UBR5 suppress spreading of chromatin ubiquitylation at damaged chromosomes. *Cell* 2012;150:697–709. <https://doi.org/10.1016/j.cell.2012.06.039>
- Gatti M, Imhof R, Huang Q *et al.* The ubiquitin ligase TRIP12 limits PARP1 trapping and constrains PARP inhibitor efficiency. *Cell Rep* 2020;32:107985. <https://doi.org/10.1016/j.celrep.2020.107985>
- Krishnan A, Speeg V, Dettwiler S *et al.* Analysis of the PARP1, ADP-ribosylation, and TRIP12 triad with markers of patient outcome in human breast cancer. *Mod Pathol* 2023;36:100167. <https://doi.org/10.1016/j.modpat.2023.100167>
- Abbasi S, Bayat L, Schild-Poulter C. Analysis of Ku70 S155 phospho-specific BioID2 interactome identifies Ku association with TRIP12 in response to DNA damage. *Int J Mol Sci* 2023;24:7041. <https://doi.org/10.3390/ijms24087041>
- Molkentine DP, Molkentine JM, Bridges KA *et al.* p16 represses DNA damage repair via a novel ubiquitin-dependent signaling cascade. *Cancer Res* 2022;82:916–28. <https://doi.org/10.1158/0008-5472.CAN-21-2101>
- Wang L, Zhang P, Molkentine DP *et al.* TRIP12 as a mediator of human papillomavirus/p16-related radiation enhancement effects. *Oncogene* 2017;36:820–8. <https://doi.org/10.1038/onc.2016.250>
- Liu X, Yang X, Li Y *et al.* Trip12 is an E3 ubiquitin ligase for USP7/HAUSP involved in the DNA damage response. *FEBS Lett* 2016;590:4213–22. <https://doi.org/10.1002/1873-3468.12471>
- Goellner EM, Svilar D, Almeida KH *et al.* Targeting DNA polymerase  $\beta$  for therapeutic intervention. *CMP* 2012;5:68–87. <https://doi.org/10.2174/1874467211205010068>
- Sobol RW, Horton JK, Kuhn R *et al.* Requirement of mammalian DNA polymerase- $\beta$  in base-excision repair. *Nature* 1996;379:183–6. <https://doi.org/10.1038/379183a0>
- Yoshizawa K, Jelezcova E, Brown AR *et al.* Gastrointestinal hyperplasia with altered expression of DNA polymerase  $\beta$ . *PLoS One* 2009;4:e6493. <https://doi.org/10.1371/journal.pone.0006493>
- Sobol RW, Foley JF, Nyska A *et al.* Regulated over-expression of DNA polymerase  $\beta$  mediates early onset cataract in mice. *DNA Repair (Amst)* 2003;2:609–22. [https://doi.org/10.1016/S1568-7864\(03\)00026-0](https://doi.org/10.1016/S1568-7864(03)00026-0)
- Prasad R, Caglayan M, Dai DP *et al.* DNA polymerase  $\beta$ : a missing link of the base excision repair machinery in mammalian mitochondria. *DNA Repair (Amst)* 2017;60:77–88. <https://doi.org/10.1016/j.dnarep.2017.10.011>
- Sykora P, Kanno S, Akbari M *et al.* DNA polymerase  $\beta$  participates in mitochondrial DNA repair. *Mol Cell Biol* 2017;37:e00237-17. <https://doi.org/10.1128/MCB.00237-17>
- Bergoglio V, Canitrot Y, Hogarth L *et al.* Enhanced expression and activity of DNA polymerase  $\beta$  in human ovarian tumor cells: impact on sensitivity towards antitumor agents. *Oncogene* 2001;20:6181–7. <https://doi.org/10.1038/sj.onc.1204743>
- Canitrot Y, Capp JP, Puget N *et al.* DNA polymerase  $\beta$  overexpression stimulates the Rad51-dependent homologous recombination in mammalian cells. *Nucleic Acids Res* 2004;32:5104–12. <https://doi.org/10.1093/nar/gkh848>
- Koczor CA, Thompson MK, Sharma N *et al.* Pol $\beta$ /XRCC1 heterodimerization dictates DNA damage recognition and basal Pol $\beta$  protein levels without interfering with mouse viability or fertility. *DNA Repair (Amst)* 2023;123:103452. <https://doi.org/10.1016/j.dnarep.2023.103452>
- Koczor CA, Saville KM, Andrews JF *et al.* Temporal dynamics of base excision/single-strand break repair protein complex assembly/disassembly are modulated by the PARP/NAD(+)/SIRT6 axis. *Cell Rep* 2021;37:109917. <https://doi.org/10.1016/j.celrep.2021.109917>
- Meng F, Wiener MC, Sachs JR *et al.* Quantitative analysis of complex peptide mixtures using FTMS and differential mass spectrometry. *J Am Soc Mass Spectrom* 2007;18:226–33. <https://doi.org/10.1016/j.jasms.2006.09.014>

39. Wiener MC, Sachs JR, Deyanova EG *et al.* Differential mass spectrometry: a label-free LC–MS method for finding significant differences in complex peptide and protein mixtures. *Anal Chem* 2004;76:6085–96. <https://doi.org/10.1021/ac0493875>
40. Braganza A, Li J, Zeng X *et al.* UBE3B is a calmodulin-regulated, mitochondrion-associated E3 ubiquitin ligase. *J Biol Chem* 2017;292:2470–84. <https://doi.org/10.1074/jbc.M116.766824>
41. An CI, Ganio E, Hagiwara N. Trip12, a HECT domain E3 ubiquitin ligase, targets Sox6 for proteasomal degradation and affects fiber type-specific gene expression in muscle cells. *Skeletal Muscle* 2013;3:11. <https://doi.org/10.1186/2044-5040-3-11>
42. Goldenberg SJ, Marblestone JG, Mattern MR *et al.* Strategies for the identification of ubiquitin ligase inhibitors. *Biochem Soc Trans* 2010;38:132–6. <https://doi.org/10.1042/BST0380132>
43. Landre V, Rotblat B, Melino S *et al.* Screening for E3-ubiquitin ligase inhibitors: challenges and opportunities. *Oncotarget* 2014;5:7988–8013. <https://doi.org/10.18632/oncotarget.2431>
44. Park Y, Yoon SK, Yoon JB. The HECT domain of TRIP12 ubiquitinates substrates of the ubiquitin fusion degradation pathway. *J Biol Chem* 2009;284:1540–9. <https://doi.org/10.1074/jbc.M807554200>
45. Chen D, Shan J, Zhu WG *et al.* Transcription-independent ARF regulation in oncogenic stress-mediated p53 responses. *Nature* 2010;464:624–7. <https://doi.org/10.1038/nature08820>
46. de Mateo S, Castillo J, Estanyol JM *et al.* Proteomic characterization of the human sperm nucleus. *Proteomics* 2011;11:2714–26. <https://doi.org/10.1002/pmic.201000799>
47. Sykora P, Witt KL, Revanna P *et al.* Next generation high throughput DNA damage detection platform for genotoxic compound screening. *Sci Rep* 2018;8:2771. <https://doi.org/10.1038/s41598-018-20995-w>
48. Reynolds P, Botchway SW, Parker AW *et al.* Spatiotemporal dynamics of DNA repair proteins following laser microbeam induced DNA damage—when is a DSB not a DSB? *Mutat Res* 2013;756:14–20. <https://doi.org/10.1016/j.mrgentox.2013.05.006>
49. Li J, MS K, Ibrahim M *et al.* NAD<sup>+</sup> bioavailability mediates PARG inhibition-induced replication arrest, intra S-phase checkpoint and apoptosis in glioma stem cells. *NAR Cancer* 2021;3:zcab044. <https://doi.org/10.1093/narcan/zcab044>
50. Georgakilas AG, O'Neill P, Stewart RD. Induction and repair of clustered DNA lesions: what do we know so far? *Radiat Res* 2013;180:100–9. <https://doi.org/10.1667/RR3041.1>
51. Chatterjee N, Walker GC. Mechanisms of DNA damage, repair, and mutagenesis. *Environ Mol Mutagen* 2017;58:235–63. <https://doi.org/10.1002/em.22087>
52. Bukowska B, Karwowski BT. The clustered DNA lesions—types, pathways of repair and relevance to Human health. *CMC* 2018;25:2722–35. <https://doi.org/10.2174/0929867325666180226110502>
53. Lomax ME, Folkes LK, O'Neill P. Biological consequences of radiation-induced DNA damage: relevance to radiotherapy. *Clin Oncol* 2013;25:578–85. <https://doi.org/10.1016/j.clon.2013.06.007>
54. Dobbs TA, Palmer P, Maniou Z *et al.* Interplay of two major repair pathways in the processing of complex double-strand DNA breaks. *DNA Repair (Amst)* 2008;7:1372–83. <https://doi.org/10.1016/j.dnarep.2008.05.001>
55. Glassner BJ, Rasmussen LJ, Najarian MT *et al.* Generation of a strong mutator phenotype in yeast by imbalanced base excision repair. *Proc Natl Acad Sci USA* 1998;95:9997–10002. <https://doi.org/10.1073/pnas.95.17.9997>
56. Mouw KW, D'Andrea AD. Crosstalk between the nucleotide excision repair and fanconi anemia/BRCA pathways. *DNA Repair (Amst)* 2014;19:130–4. <https://doi.org/10.1016/j.dnarep.2014.03.019>
57. Fujii S, Sobol RW, Fuchs RP. Double-strand breaks: when DNA repair events accidentally meet. *DNA Repair (Amst)* 2022;112:103303. <https://doi.org/10.1016/j.dnarep.2022.103303>
58. Cheng X, An J, Lou J *et al.* Trans-lesion synthesis and mismatch repair pathway crosstalk defines chemoresistance and hypermutation mechanisms in glioblastoma. *Nat Commun* 2024;15:1957. <https://doi.org/10.1038/s41467-024-45979-5>
59. Raaphorst GP, Cybulski SE, Sobol R *et al.* The response of human breast tumour cell lines with altered polymerase  $\beta$  levels to cisplatin and radiation. *Anticancer Res* 2001;21:2079–83.
60. Neijenhuis S, Verwijs-Janssen M, Kasten-Pisula U *et al.* Mechanism of cell killing after ionizing radiation by a dominant negative DNA polymerase  $\beta$ . *DNA Repair (Amst)* 2009;8:336–46. <https://doi.org/10.1016/j.dnarep.2008.11.008>
61. Vermeulen C, Verwijs-Janssen M, Begg AC *et al.* Cell cycle phase dependent role of DNA polymerase  $\beta$  in DNA repair and survival after ionizing radiation. *Radiother Oncol* 2008;86:391–8. <https://doi.org/10.1016/j.radonc.2008.01.002>
62. Vermeulen C, Verwijs-Janssen M, Cramers P *et al.* Role for DNA polymerase  $\beta$  in response to ionizing radiation. *DNA Repair (Amst)* 2007;6:202–12. <https://doi.org/10.1016/j.dnarep.2006.09.011>
63. Kajiro M, Tsuchiya M, Kawabe Y *et al.* The E3 ubiquitin ligase activity of Trip12 is essential for mouse embryogenesis. *PLoS One* 2011;6:e25871. <https://doi.org/10.1371/journal.pone.0025871>
64. David R. DNA damage response: restricting repair. *Nat Rev Mol Cell Biol* 2012;13:601. <https://doi.org/10.1038/nrm3437>
65. Zhang J, Gambin T, Yuan B *et al.* Haploinsufficiency of the E3 ubiquitin-protein ligase gene TRIP12 causes intellectual disability with or without autism spectrum disorders, speech delay, and dysmorphic features. *Hum Genet* 2017;136:377–86. <https://doi.org/10.1007/s00439-017-1763-1>
66. O'Roak BJ, Stessman HA, Boyle EA *et al.* Recurrent *de novo* mutations implicate novel genes underlying simplex autism risk. *Nat Commun* 2014;5:5595. <https://doi.org/10.1038/ncomms6595>
67. Onishi K, Uyeda A, Shida M *et al.* Genome stability by DNA polymerase  $\beta$  in neural progenitors contributes to neuronal differentiation in cortical development. *J Neurosci* 2017;37:8444–58. <https://doi.org/10.1523/JNEUROSCI.0665-17.2017>
68. Fang Q, Andrews J, Sharma N *et al.* Stability and sub-cellular localization of DNA polymerase  $\beta$  is regulated by interactions with NQO1 and XRCC1 in response to oxidative stress. *Nucleic Acids Res* 2019;47:6269–86. <https://doi.org/10.1093/nar/gkz293>
69. Sobol RW, Prasad R, Evenski A *et al.* The lyase activity of the DNA repair protein  $\beta$ -polymerase protects from DNA-damage-induced cytotoxicity. *Nature* 2000;405:807–10. <https://doi.org/10.1038/35015598>
70. Whitehouse CJ, Taylor RM, Thistlethwaite A *et al.* XRCC1 stimulates human polynucleotide kinase activity at damaged DNA termini and accelerates DNA single-strand break repair. *Cell* 2001;104:107–17. [https://doi.org/10.1016/S0092-8674\(01\)00195-7](https://doi.org/10.1016/S0092-8674(01)00195-7)
71. Srivastava DK, Husain I, Arteaga CL *et al.* DNA polymerase  $\beta$  expression differences in selected human tumors and cell lines. *Carcinogenesis* 1999;20:1049–54. <https://doi.org/10.1093/carcin/20.6.1049>
72. Li M, Zang W, Wang Y *et al.* DNA polymerase  $\beta$  promoter mutations and transcriptional activity in esophageal squamous cell carcinoma. *Tumor Biol* 2013;34:3259–63. <https://doi.org/10.1007/s13277-013-0898-5>
73. Dong ZM, Zheng NG, Wu JL *et al.* Difference in expression level and localization of DNA polymerase  $\beta$  among human esophageal cancer focus, adjacent and corresponding normal tissues. *Dis Esophagus* 2006;19:172–6. <https://doi.org/10.1111/j.1442-2050.2006.00560.x>
74. Yu J, Mallon MA, Zhang W *et al.* DNA repair pathway profiling and microsatellite instability in colorectal cancer. *Clin Cancer Res* 2006;12:5104–11. <https://doi.org/10.1158/1078-0432.CCR-06-0547>
75. Fan R, Kumaravel TS, Jalali F *et al.* Defective DNA strand break repair after DNA damage in prostate cancer cells: implications for



- genetic instability and prostate cancer progression. *Cancer Res* 2004;**64**:8526–33.  
<https://doi.org/10.1158/0008-5472.CAN-04-1601>
76. Ramakodi MP, Devarajan K, Blackman E *et al.* Integrative genomic analysis identifies ancestry-related expression quantitative trait loci on DNA polymerase  $\beta$  and supports the association of genetic ancestry with survival disparities in head and neck squamous cell carcinoma. *Cancer* 2017;**123**:849–60.  
<https://doi.org/10.1002/cncr.30457>
  77. Park Y, Yoon SK, Yoon JB. TRIP12 functions as an E3 ubiquitin ligase of APP-BP1. *Biochem Biophys Res Commun* 2008;**374**:294–8. <https://doi.org/10.1016/j.bbrc.2008.07.019>
  78. Chen D, Yoon JB, Gu W. Reactivating the ARF-p53 axis in AML cells by targeting ULF. *Cell Cycle* 2010;**9**:3018–23.  
<https://doi.org/10.4161/cc.9.15.12355>
  79. Collado M, Serrano M. The TRIP from ULF to ARF. *Cancer Cell* 2010;**17**:317–8. <https://doi.org/10.1016/j.ccr.2010.03.015>
  80. Doil C, Mailand N, Bekker-Jensen S *et al.* RNF168 binds and amplifies ubiquitin conjugates on damaged chromosomes to allow accumulation of repair proteins. *Cell* 2009;**136**:435–46.  
<https://doi.org/10.1016/j.cell.2008.12.041>
  81. Lan L, Nakajima S, Wei L *et al.* Novel method for site-specific induction of oxidative DNA damage reveals differences in recruitment of repair proteins to heterochromatin and euchromatin. *Nucleic Acids Res* 2014;**42**:2330–45.  
<https://doi.org/10.1093/nar/gkt1233>
  82. Eccles LJ, Menoni H, Angelov D *et al.* Efficient cleavage of single and clustered AP site lesions within mono-nucleosome templates by CHO-K1 nuclear extract contrasts with retardation of incision by purified APE1. *DNA Repair (Amst)* 2015;**35**:27–36.  
<https://doi.org/10.1016/j.dnarep.2015.08.003>
  83. Ulrich HD, Walden H. Ubiquitin signalling in DNA replication and repair. *Nat Rev Mol Cell Biol* 2010;**11**:479–89.  
<https://doi.org/10.1038/nrm2921>
  84. Huang TT, D'Andrea AD. Regulation of DNA repair by ubiquitylation. *Nat Rev Mol Cell Biol* 2006;**7**:323–34.  
<https://doi.org/10.1038/nrm1908>
  85. Schwertman P, Bekker-Jensen S, Mailand N. Regulation of DNA double-strand break repair by ubiquitin and ubiquitin-like modifiers. *Nat Rev Mol Cell Biol* 2016;**17**:379–94.  
<https://doi.org/10.1038/nrm.2016.58>
  86. Chitale S, Richly H. Timing of DNA lesion recognition: ubiquitin signaling in the NER pathway. *Cell Cycle* 2017;**16**:163–71.  
<https://doi.org/10.1080/15384101.2016.1261227>
  87. Harreman M, Taschner M, Sigurdsson S *et al.* Distinct ubiquitin ligases act sequentially for RNA polymerase II polyubiquitylation. *Proc Natl Acad Sci USA* 2009;**106**:20705–10.  
<https://doi.org/10.1073/pnas.0907052106>